ENGINEERING RESEARCH INSTITUTE
UNIVERSITY OF MICHIGAN
ANN ARBOR

FINAL REPORT

HIGH RESOLUTION AUTORADIOGRAPHY FOR STUDY OF GRAIN BOUNDARIES IN METALS

By

H. J. GOMBERG
M. J. SINNOTT
C. UPTHEGROVE
R. A. FLINN
L. H. VAN VLACK
S. YUKAWA
A. S. KEH
H. B. PROBST
R. SIMONSEN
G. C. TOWE
C. M. HAMMOND

Project 2029

U. S. ARMY ORDNANCE CORPS
CONTRACT NO. DA-20-018-ORD-12150, PROJECT NO. TB-121
(DA PROJECT 593-08-023) WAL 843/13-19

February, 1954

SUMMARY SHEET

a. Engineering Research Institute, University of Michigan

b. U. S. Army, Ordnance Corps

c. O. O. Project No. TB4-121, Contract DA-20-018 ORD-12150

d. WAL Report No. 843/13-10

e. Priority No.: None

f. High-Resolution Autoradiography for Study of Grain Boundaries in Metals

g. Object:

The research work under this contract is to be devoted to the development and use of high-resolution autoradiography for the study of grain boundaries of metals. Specifically, the objects are (1) to improve the wet-collodion technique for autoradiography to permit application to the study of metallic systems; (2) to develop protective coatings of optimum thinness to prepare metals for autoradiography; (3) to use various radioisotopes, including emitters of both high- and low-energy radiations, for autoradiographic purposes and to develop methods for incorporating them into metals; and (4) to apply the techniques developed to the investigation of grain-boundary constituents in alloy systems that contain iron and the other transitional elements, and also to other types of alloys.

h. Summary:

Equipment and procedures used for the autoradiography study of metallurgical problems are presented in this report. Results are given showing that high-resolution autoradiography methods can be a very valuable tool in the study of such problems as the diffusion of nickel into iron and into copper, diffusion of bismuth into copper, distribution of bismuth in copper, identification and distribution of sulfides in iron, distribution of hydrogen in copper-tin alloys, and distribution of sulfur in cast irons. Factors that should be considered in the interpretation and evaluation of autoradiographs are also discussed.

i. Conclusions and Recommendations:

High-resolution autoradiography can be used for microstructural analysis in metallurgy. Results show that a resolution of 10 microns or better is readily possible. Some new information, as well as substantiation of known facts about the systems investigated, have been obtained through the use of autoradiographic techniques.

It is recommended that the studies of the application of high-resolution autoradiography to metallurgy be continued.

DISTRIBUTION LIST

No. of Copies	
2	Chief of Ordnance Department of the Army Washington 25, D. C. Attention: ORDTB-Research and Materials
1	Chief of Ordnance Department of the Army Washington 25, D. C. Attention: ORDTX-AR-Executive Library
1	Chief of Ordnance Department of the Army Washington 25, D. C. Attention: ORDIX
2	Commanding Officer Frankford Arsenal Bridesburg Station Philadelphia 37, Pennsylvania
1	Commanding Officer Picatinny Arsenal Dover, New Jersey
1	Commanding Officer Rock Island Arsenal Rock Island, Illinois
1	Commanding Officer Springfield Armory Springfield 1, Massachusetts
1	Commanding Officer Watervliet Arsenal Watervliet, New York
2	Commanding Officer Detroit Arsenal Center Line, Michigan

DISTRIBUTION LIST (continued)

No. of Copies	
2	Commanding General Redstone Arsenal Huntsville, Alabama
2	Commanding General Aberdeen Proving Ground Aberdeen, Maryland Attention: ORDBG, RD and E Library
1	Commanding Officer Office of Ordnance Research Box CM, Duke Station Durham, North Carolina
1	Chief, Bureau of Aeronautics Navy Department Washington 25, D. C.
1	Chief, Bureau of Ordnance Navy Department Washington 25, D. C.
1	Chief, Bureau of Ships Navy Department Washington 25, D. C. Attention: Code 324
1	Director, Naval Research Laboratory Anacostia Station Washington 25, D. C.
1	Chief, Office of Naval Research Navy Department Washington 25, D. C.
1	Commanding Officer Naval Proving Ground Dahlgren, Virginia Attention: A and P Laboratory
1	Chief, Naval Experimental Station Navy Department Annapolis, Maryland

No. of Copies	
1	Commanding General Wright Air Development Center Wright-Patterson Air Force Base Dayton, Ohio Attention: WCRTO
1	Commanding General Wright Air Development Center Wright-Patterson Air Force Base Dayton, Ohio Attention: WCRRL
1	National Advisory Committee for Aeronautics 1724 F. Street, N. W. Washington 25, D. C.
3	U. S. Atomic Energy Commission Technical Information Service P. O. Box 62 Oak Ridge, Tennessee Attention: Chief, Library Branch
3	U. S. Atomic Energy Commission 1901 Constitution Avenue Washington 25, D. C. Attention: Chief, Library Branch
5	Commanding Officer Watertown Arsenal Watertown 72, Massachusetts Attention: ORDBE-L
1	Director, Ordnance Materials Research Office c/o Watertown Arsenal Watertown 72, Massachusetts
1	District Chief Detroit Ordnance District 574 East Woodbridge Detroit 31, Michigan
5	Document Service Center Armed Servies Technical Information Agency Knott Building Dayton 2, Ohio Attention: DSC-SD2

TABLE OF CONTENTS

TABLE OF CONTENTS (CONCLUDED)

LIST OF FIGURES

LIST OF FIGURES (CONCLUDED)

ABSTRACT

This report presents the results obtained from experimental work directed toward (1) improvements in the techniques of high-resolution autoradiography, and (2) application of the autoradiographic techniques in studies of metallurgical problems.

Of the several available methods of high-resolution autoradiography, the stripping-film method is the simplest and most consistent in execution and results. Recommended procedures for sample preparation, application of plastic protective coating, application of the stripping film, exposure conditions, and processing of the autoradiographs are given. One of the most troublesome difficulties of stripping-film autoradiography, namely peeling, buckling, and shifting of the emulsion during exposure and processing, has been practically eliminated by the addition of a wetting agent to the water used during the application operation.

Along with techniques, the radioactive characteristics of isotopes desirable for high-resolution autoradiography and factors that should be considered in the interpretation of autoradiographs are discussed.

A number of widely different types of metallurgical problems were studied using the autoradiographic technique in order to evaluate its usefulness is a metallurgical research tool. These problems included the following:

1. diffusion of nickel into iron,
2. distribution of sulfides in iron,
3. distribution of bismuth in copper,
4. diffusion of liquid bismuth into copper,
5. diffusion of nickel into copper,
6. distribution of hydrogen (tritium) in copper-tin alloys, and
7. distribution of sulfur in cast iron with spherulitic graphite.

A description of procedures and equipment used for the introduction of the radioactive isotopes and the subsequent steps of heat treatment, sample preparation, etc., is given for each of these systems.

The value of high-resolution autoradiography as a metallurgical research tool is amply demonstrated by the results obtained. Some new information about these metallic systems, as well as substantiation of known facts, have been obtained.

Autoradiographs showing the diffusion of nickel along grain boundaries or iron in both the gamma and alpha-phase regions and some quantitative data for the extent of this diffusion are given. Autoradiographic identification and differentiation of sulfides in iron is shown,

as well as a quantitative estimate of the width of a sub-microscopic film of sulfide, if it exists. The autoradiographic pattern of bismuth distribution in copper is correlated with the subgrain structure, and the absence of any change in this distribution with subsequent metallurgical operations is noted. The influence of relative crystal orientation on the extent of grain-boundary diffusion of both bismuth and nickel into copper has been studied using autoradiographs to aid in identifying the diffusion material in the grain boundaries. Microstructural and autoradiographic evidence of tritium absorption by copper-tin alloys during melting indicates that tritium, and presumably ordinary hydrogen, is generally distributed in a very loosely bound state in this alloy. No conclusive evidence was found regarding the distribution of sulfur in cast irons.

FOREWORD

This report contains the results of a research program conducted to investigate the application of autoradiography to the study of metallurgical problems. The research program was directed toward two main objectives: first, the development and refinement of the autoradiographic technique so that it can be used as a reliable experimental tool, and second, study of several distinctly different metallurgical systems by the autoradiographic technique to evaluate its capabilities and limitations.

The report has been divided into two main sections based on these two objectives. The first section contains a discussion of radioactivity and its detection, the unique value of autoradiography as a means of detection; and a description of the techniques of making autoradiographs of metallic samples. The second section includes descriptions of experimental methods used in making radioactive specimens for each of the systems studied and the autoradiographic results obtained. Metallurgical phenomena studied include diffusion, gases in metals, effect of heat treatment on mode of distribution of a minute phase, and the modifying effects of trace quantities of an element on the formation of a second constituent.

The use of the facilities and the cooperation and efforts of Mr. David E. Weyant of the Radioactive Isotopes Laboratory of the Michigan Memorial Phoenix Project were particularly helpful throughout this research program and are gratefully acknowledged. Also, many valuable suggestions and advice on autoradiographic techniques were received from the personnel of the Atomic Energy Commission research project on High-Resolution Autoradiography.

FINAL REPORT

HIGH-RESOLUTION AUTORADIOGRAPHY FOR STUDY OF GRAIN BOUNDARIES IN METALS

AUTORADIOGRAPHY

Radioactivity

In the last few years a great many new isotopes of the elements have become available. Almost all these new isotopes are radioactive; i.e., they are unstable and will, at some time, become converted to another isotope of the same or a different element. This process of conversion, or radioactive decay, is always accompanied by emission of some type of radiation. When the radiation emitted is an electron, the isotope is called a beta emitter. In the same way, an alpha emitter radiates alpha particles (the nuclei of helium atoms) and gamma emitters radiate photons.

Chemically and physically, these radioactive isotopes before decay behave identically with the more familiar stable isotopes of the elements. If radioactive isotopes are introduced into a metallic system, their location can be determined later by detecting and locating the source of radiation. For the metallurgist, this provides a means of locating and following the movement of atoms in metals under the influence of various processing and heat treatments. This use of radioactivity is known as the radioactive tracer technique.

The ultimate value of a radioactive tracer technique depends on the sensitivity and the spatial resolution of the detectors used in locating the radiation sources. Sensitivity refers to the minimum amount of radioactivity necessary to produce an observable effect in the detector, while resolution denotes the minimum spacing between the sources that the detector is capable of differentiating. Of all the radiation detection methods that are now available, autoradiography has the highest resolution. Since most metallurgical problems involve examinations and observations on a micro-

scopic scale, the value of autoradiography as an experimental tool in metallurgy is very great.

Autoradiographic Methods

Essentially, autoradiography refers to a method of detecting radioactivity where the emitted radiations are used to produce a "picture" in much the same manner that sunlight is used to produce a "picture" in ordinary photography. The radiation-sensitive materials most often used is the silver-halide type of photographic emulsion. The several different methods of autoradiography differ mostly in the manner of bringing the emulsion in close contact with the metal surface which contains the radioactivity.

The various methods of autoradiography have been described previously in the Interim Report of February, 1953, and only a short summary of that discussion will be presented here for convenient reference.

1. Contact Autoradiography: The specimen is simply laid on the photographic film: The film is processed and examined detached from the specimen. The process has inherently low resolution but is very simple in execution.

2. Stripping-Film Autoradiography: A thin emulsion is stripped from a backing material and placed on a specimen. The emulsion is processed and examined intact with the specimen. This process is capable of high resolution and is fairly simple in execution.

3. Painted-Emulsion Autoradiography: The emulsion is heated to the liquid state and painted on the specimen surface, and then processed and examined intact with the specimen. Characteristics of the process are variable sensitivity and high background.

4. Wet-Process Autoradiography: A sensitive silver bromide layer is formed chemically on the specimen surface; thickness can be controlled. The emulsion layer is processed and examined intact with the specimen. This process is potentially capable of the highest resolution but is more complicated and sensitive in execution than the other methods.

Of the high-resolution methods, the stripping-film method has been used on a routine basis in this research program and the wet-process method only when higher resolutions were required.

Radioactivity Considerations for Autoradiography

The mere fact that an isotope is radioactive does not mean that it can be used as a tracer in an investigation of a metallurgical problem by autoradiographic techniques. Isotopes of a fairly large number of the elements are known, but many of them are not suitable for use in autoradiography. Among the factors to be considered in determining the suitability of an isotope are the type of radiation, half-life, decay scheme, and radiochemical purity.

For high-resolution autoradiography the ideal isotopes are the low-energy beta emitters. Both theoretical and experimental work in the field of high-resolution autoradiography has shown that resolution is improved by (1) close contact of emulsion to specimen surface, (2) thin emulsion, and (3) thin specimens. Assuming that the first two of these factors are constant, the effective thickness of a specimen is reduced as the energy of radiation is decreased. The reason for this is that the depth of subsurface radiations is reduced as the energy of radiation becomes lower; therefore, higher resolutions are inherently possible with low-energy radiations because the blackening over a specific radioactive source is sharper. Furthermore, low-energy beta-emitting isotopes are much more convenient to handle from the standpoint of health physics.

The high penetrating power of gamma radiations severely limits the usefulness of gamma emitters in high-resolution autoradiography for the reason mentioned above. It is possible to circumvent this difficulty by using very thin specimens; however, the handling problems remain.

Although the energy of alpha radiations from most alpha-emitting isotopes is quite high, their penetrating power is relatively low. For this reason, the problem of subsurface radiations is not as great. Also, alpha radiations produce characteristic tracks in the emulsion, and by tracing these tracks back to their origin, it is possible to locate very precisely the source of radiation.

Many isotopes emit several types of radiations simultaneously. These isotopes can be used for high-resolution work in certain cases; e.g., when the emitted radiation is mainly low-energy beta particles with some gamma radiation. The response of thin emulsions, e.g., stripping film, is about a thousand times greater for beta than for gamma radiations. Thus, in effect, very little of the gamma radiation is detected by the emulsion. Along the same line, the response of the emulsion to alpha radiations is about a thousand times greater than for beta radiations.

A very important factor in determining the suitability of an isotope for autoradiography is its half-life. Obviously, if the half-life is too short, there is no time to introduce the isotope into a metallic system

and to process it before the activity is reduced to so low a level as to be of no value. For this reason two isotopes of particular interest in metallurgy, namely oxygen and nitrogen, cannot be used for autoradiography.

The decay scheme of many isotopes involves going from one radioactive isotope to another. For example, bismuth-210 is a beta emitter; the daughter of this decay, polonium-210 is an alpha emitter and half-lives are 5 and 138 days respectively. The alpha activity of the polonium practically masks all the beta activity of the bismuth; some of the problems connected with this will be discussed later in this report in connection with a specific use of this isotope. In determining suitability for autoradiography, each isotope having this decay scheme has to be considered individually, depending on the activity, half-life, and type of radiation of the parent and the daughter.

Even though all the other characteristics of an isotope are favorable, it may not be satisfactory for autoradiographic work if its radiochemical purity is not high. Many isotopes cannot be produced free of contamination nor can they be separated subsequently. These contaminations may be another isotope of the same element or an isotope of some trace impurity element in the target material.

Autoradiographic Procedures

Contact Autoradiography. The experimental procedure used to make the few contact autoradiographs obtained during the course of this research is very simple. A sample of the metal containing the radioactivity is given a metallurgical polish and then placed on a photographic plate or film. The plate specimen assembly is placed in a light-tight box and exposed for the desired time. Processing procedures were exactly as prescribed for the plate or film used.

There is at present no reliable way of determining the exposure time required except by trial and error. In most metallurgical studies, several specimens can be obtained from the same piece. Several autoradiographic exposures can be started simultaneously and then processed at increasing exposure times. Alternatively, if the isotope has a long half-life, a series of autoradiographs of the same specimen differing in exposure time can be made. A suggested starting point would be an exposure time of 1 day, although this is dependent on many factors.

Stripping-Film Autoradiography. The stripping films made by both the American and British Kodak firms were tried, but best results were obtained with the American Kodak product. The designation used by Eastman Kodak for their product is Experimental Permeable Base Autoradiographic Stripping Film. The unused portions of the stripping film have been kept

in a refrigerator and deterioration appears to be no problem at all. The same roll of film used 5 to 6 months later has produced successful autoradiographs.

The surface preparation used is exactly the same as would be used for an ordinary metallurgical examination. In polishing the specimen, care must be taken to avoid smearing any radioactive material across the surface. If an etchant is used, careful washing is necessary to remove any etchant entrapped in cracks, structural porosities, etc. Autoradiographs have been made of both etched and unetched surfaces.

Since the emulsion is processed intact with the specimen in stripping-film autoradiography, it is necessary to protect the specimen surface from corrosion by the developing and fixing solutions. Several different kinds of protective plastic coatings were tried and the most satisfactory results were obtained with a 2% solution of vinylite (Bakelite designation: VYNS) in methyl-ethyl ketone. This solution tends to dissolve some of the bakelite mounting if the mount curing temperature is too low. Curing the mounts at around 135°C eliminates this problem. The mounted and polished specimen is immersed in the plastic solution for about 15 seconds. The specimen is then removed from the plastic solution and held vertically so that the excess solution drains down across the face of the specimen. After air drying for 2 minutes, the specimen is placed face-up under a heat lamp to harden the plastic coating. With a lamp placed approximately 18 inches from the specimen, a baking time of 30 minutes to 1 hour is sufficient. When the specimen has cooled, it is ready for the application of the stripping film.

There are several possible ways that the stripping film may be applied, but the procedure described below was found to be the easiest. Since the whole operation of applying the stripping film must be done in a darkroom with only a red safelight, only practice can develop proficiency; the following is just a general step-by-step outline of the operation:

1. Lay the specimen mount face-up and make a pool of water on the surface of the specimen. About 1% of sodium lauryl sulfate (Dupanol "C") is added to the water as a wetting agent.

2. Cut a piece of stripping film from the roll. The size should be slightly larger than one-half of the final size desired, since the emulsion swells during application.

3. With a pair of tweezers, strip the emulsion away from the backing material and float it on the pool of water.

4. Allow the emulsion to float on the water for about 1 minute, during which time it will soak up some water.

5. Carefully remove the water by soaking it up with pieces of filter paper. The emulsion can be positioned over a desired area of the sample by proper choice of the direction of removing the water.

6. Any water remaining trapped under the emulsion can be removed by slightly tilting the mount so that the water collects to one side, where it can be soaked up with filter paper.

Photographs illustrating some of these steps are shown in Fig. 1

By this procedure, the emulsion is slowly settled onto the specimen surface, insuring good contact between them. The specimen with the adhering emulsion is stored in a light-tight box for the desired exposure time.

The exposure time is best determined by making a series of autoradiographs of varying exposure times in the manner described for contact autoradiography.

After exposure, the emulsion is processed without removal from the specimen, by immersing the whole specimen mount in the developer, fixer, and wash water. The solutions and times used for the various processing steps are as follows:

Developer: Kodak D-19 diluted 1 part stock solution to 2 parts distilled; time, 90 seconds.

Stop Bath: Distilled water; time, 3-4 seconds.

Fixer: Ordinary hypo fixer such as Kodak F-5; time, 2 minutes.

Wash: Distilled water; time, 10 minutes.

After removing from the wash water and drying, the autoradiograph is ready for examination.

In the early part of this research program, a great deal of difficulty was experienced due to cracking and peeling of the emulsion during the exposure period. This difficulty, as well as the associated problem of film shifting during processing, have been nearly eliminated by the use of the wetting agent in the water for applying the emulsion.

Some of the difficulties of cracking and peeling are dependent on storage conditions during exposure. Ordinary room conditions are satisfactory if the humidity is not too low. During the summer months, large variations in humidity from day to day cause the most trouble in this respect. When the film is applied using the wetting agent mentioned previously, it was found that a refrigerator can also be used for storage. The background can be reduced somewhat by storing at the lower temperature, but the sensitivity of the emulsion is probably also reduced to some extent.

Wet-Process Autoradiography. This method is far more complicated and sensitive to the processing variables than the stripping-film method. For this reason, the wet-process method was attempted in this research program only when it was felt that its inherently higher resolution was required. Although Towe[1] has obtained excellent results by this method, no completely satisfactory wet-process autoradiograph was obtained with any of the metallic systems investigated here.

Since a very complete description of the techniques of wet-process autoradiography is given by Gomberg[2] and its application to metallurgical samples is discussed in a forthcoming publication[1], this material will not be repeated here.

Interpretation of Autoradiographs

A great deal of care and caution should be exercised in interpreting and evaluating the autoradiographs to avoid erroneous conclusions. Many factors during the various stages of applying, exposing, and processing autoradiographs can produce results which can be mistakenly attributed to radioactivity.

The most common and obvious of these factors is the background or fog of any photographic emulsion. The contributing sources of background are many and varied; some of them are inherent in the emulsion itself. Other sources are cosmic radiations, stray radiations normally present around any laboratory, light leaks, etc. The problem of fog becomes especially important when the radioactivity is distributed uniformly in the specimen. If the activity level of the specimen is low, it is often quite difficult to separate the radioactive response from the background.

Another type of extraneous background which is even more troublesome than uniform fogging is the localized type. This problem seems to arise from localized straining or bending of the emulsion during application. In the completed autoradiograph, it shows up as streaks of developed silver grains. Although this type of background can usually be identified as being due to extraneous sources because the streaks are

generally quite straight, they are nevertheless very annoying. The streaks can occur over areas of interest and obscure any silver grains which may have been activated by radioactivity.

Artifacts due to chemical corrosion constitute another very serious difficulty. As mentioned before, a protective plastic film is applied over the specimen surface to prevent corrosion. However, the plastic is not always completely impervious to moisture and processing solutions. Furthermore, it seems that this plastic breakdown is dependent on the metallurgical structure of the specimen. A homogeneous structure is less likely to produce this difficulty. In a heterogeneous structure, the different phases always polish more or less in relief and the plastic film sometimes ruptures in stretching over the ridges. For this reason, porosity should be kept to a minimum in specimens used for autoradiographic studies.

Chemical corrosion resulting from plastic breakthrough can very often activate the silver grains in exactly the same manner and pattern that radioactivity does. Therefore, any apparent radioactivity over areas where there is no underlying structural component to account for the radioactivity should be regarded with suspicion.

Although largely eliminated now, there were some difficulties of a mechanical nature in the stripping-film method, such as the problem of film shifting, peeling, and buckling during processing. The use of a wetting agent in the water during application seems to have solved this problem.

Some of the autoradiographs shown later in this report will illustrate the points mentioned above regarding the interpretation of autoradiographs.

From the foregoing discussion, it is easy to recognize the importance of using control samples in all autoradiographic work to eliminate ambiguity concerning response to radioactivity. The control sample should be identical as far as possible in all ways to the radioactive samples and should be polished, etched, autoradiographed, and processed in the same way.

METALLURGICAL APPLICATIONS

A proper evaluation of the role of autoradiography as a research tool in metallurgy can be made only after using it in the study of

specific metallurgical problems. The research program conducted included a number of widely different metallic systems and phenomena, but there was one objective common to all of them, namely the location and identification of a microscopic or submicroscopic phase or concentration of atoms.

In the field of metallic diffusion, the grain-boundary diffusion of nickel into iron, nickel into copper, and liquid bismuth into copper was investigated. The identification of sulfides in iron constitutes an example of identifying a minute grain-boundary phase. The problem of gases in metal has been studied by using tritium with copper-base alloys. Investigations using bismuth in cast and recrystallized copper and sulfur in cast iron containing spherulitic graphite are typical of problems which involve determining the distribution of impurity and alloying elements in metals.

DIFFUSION OF NICKEL INTO IRON

Introduction

Nickel and iron are similar in structure (face-centered cubic) at the higher temperatures and form solid solutions in all proportions. Previous investigations of diffusion of nickel in iron have come to differing conclusions concerning the occurrence of grain-boundary diffusion for this diffusion couple. Wells and Mehl[3] found no evidence of grain-boundary diffusion of nickel into low-carbon iron and steel. Kuczynski and Alexander[4], on the other hand have reported observing diffusion along grain boundaries. In the Interim Report of February, 1953, for this project, some preliminary results on the investigation of this system were reported in which it was indicated that grain-boundary diffusion could occur. Further experiments have been carried out using radioactive nickel to substantiate these preliminary findings.

Nickel-63, a radioactive isotope of nickel, has very desirable characteristics from an autoradiographic standpoint. Its radiation consists of low-energy (0.06 mev) beta particles only, and it has a long half-life (85 years). The maximum range of the emitted beta particle in steel is about 8 microns. It is a relatively safe isotope to handle, and the long half-life means that the loss of activity during an experiment is negligible.

Experimental Procedure

Material. The radioactive nickel used was obtained from the Atomic Energy Commission and had the following specifications:

Catalog No.: Ni-63 (28-P)
Specific Activity: 9.7 mc/gm
Chemical Form: $NiCl_2$ in 0.0286N HCl
Nickel Content: 75 mg/ml
Impurities: Hg^{203}, 0.01%
Total Volume: 5.5 ml

The iron was vacuum-melted iron (Ferrovac) obtained from the Vacuum Metals Corporation with the following composition:

Carbon: 0.005%
Oxygen: 0.0037%
Nitrogen: 0.00008%
Iron: Balance

The iron was supplied in the form of 1/2-inch-diameter rods and disks 1/8-inch thick were cut from this rod and used as the diffusion specimens.

Chemical Purification of Nickel. Attempts to electroplate a thin layer of radioactive nickel using procedures initially worked out with stable nickel indicated that some impurity in the solution of radioactive nickel was interfering with the plating process. Therefore, the solution obtained from the Atomic Energy Commission was purified in the manner described below.

Hydrogen sulfide was bubbled into the solution to precipitate any elements forming insoluble sulfides in an acid solution. A trace of a black precipitate obtained by this treatment was removed by filtering. The precipitate was washed with water containing hydrogen sulfide. Monitoring this precipitate showed that it was radioactive, indicating that it was probably mercury. Hydrogen peroxide was added to the filtrate and the solution carefully boiled to reoxidize to the trivalent state any iron which might be present.

The solution was diluted to 200 ml with water, 0.5 gm of citric acid added, and the solution made slightly acidic with hydrochloric acid; then 3 gm of dimethylglyoxime dissolved in 80 ml of hot alcohol was added and the solution was heated, producing some precipitation of nickel dimethylglyoxime. The precipitation was completed by making the solution slightly basic with ammonium hydroxide. The precipitate was allowed to settle by keeping the solution warm for 1 hour and then filtered on a fritted-glass filtering funnel and washed with water containing some ammonium hydroxide. Tests on the filtrate indicated that all the nickel had been precipitated.

The precipitate was redissolved without removal from the funnel by pouring over it a solution consisting of 15 ml nitric acid, 15 ml hydrochloric acid, and 20 ml of 1:1 sulfuric acid. The solution was evaporated to dryness and nitric acid added dropwise to the fuming residue until all organic matter was destroyed. The salts were dissolved in 100 ml of water and then evaporated back to the original volume of 5.5 ml.

All these operations were performed under a hood with proper precautions for radiological safety.

Electroplating Procedure. In order to simplify the plating of radioactive nickel, a special electroplating cell (Fig. 2) was designed and constructed. Use of this cell reduces the handling of the radioactive solution to a minimum.

The iron specimens were prepared for plating by a preliminary surface grinding, followed by hand polishing on fine emery paper, and acid pickling.

The nickel was plated from an ammoniacal sulfate solution obtained by adding ammonium hydroxide to the purified solution until a deep blue color resulted.

A plate of radioactive nickel approximately 0.001-inch thick was produced by plating for 10 minutes at a current density of 13 milliamperes per sq cm. The plate appeared smooth and continuous with good adhesion.

Prior Heat Treatment of Iron. Most of the diffusion studies were made on iron in the as-received cold-drawn condition. However, in the course of the investigation, it appeared that prior heat treatment might have some influence on the pattern of grain-boundary diffusion that was being observed.

The heat treatment consisted of vacuum-annealing at 2000°F for 20 hours followed by a slow furnace-cooling. A very coarse alpha-iron grain size resulted from this treatment.

Diffusion Anneal. The diffusion of nickel into iron was investigated mainly at 1800°F where the iron is in the gamma (face-centered-cubic) phase. Several runs were made at 1350 and 1100°F to investigate diffusion in this system when the iron is in the alpha (body-centered cubic) phase.

The diffusion runs were made by sealing the specimens under vacuum in Vycor glass capsules. The sealed specimens were then placed in a tubular furnace already maintained at the diffusion temperature. At the end of a

run, the capsule was quickly removed from the furnace, plunged into water, and broken underwater.

No evidence of iron oxidation was observed on any specimen, which indicates that a satisfactory vacuum was maintained during the diffusion run.

Specimen Examination. After the diffusion anneal the specimens were cut in half perpendicular to the diffusion interface. Conventional metallographic techniques of grinding and polishing the mounted specimens were used, the final polishing being done with Gamal.

Experimentation with several etching reagents revealed that the grain-boundary diffusion could best be shown by an etchant mixed in the proportions of 15 ml nitric acid and 10 ml acetic acid to 50 ml of water.

Autoradiographs were made using procedures previously outlined.

Results

Metallographic. Preliminary to making an autoradiographic study of the diffusion of nickel into iron, a series of specimens was run using stable nickel under conditions identical to those used for the radioactive series. Metallographic evidence of grain-boundary diffusion was found even for diffusion times as short as 5 hours at 1800°F. On etching, "fingers" of nickel penetration into the iron could be observed. Near the interface, these "fingers" often completely enveloped the iron grains. At increasing distance from the interface the spacing between these "fingers" becomes wider. Depending on the diffusion time, a point is reached where the concentration of nickel in the "fingers" becomes so low that positive metallographic identification is difficult. Thus, the end point of nickel penetration cannot be determined satisfactorily by metallographic examination alone.

The influence of diffusion times of up to 338 hours was investigated in this series of specimens using the stable nickel. Examination of these longer-diffusion-time specimens showed that some of the iron grains enveloped by the nickel "fingers" had a Widmanstatten structure. The depth to which this effect was observed increased with increasing diffusion times. Evidently this is the result of volume diffusion of nickel into the matrix of the iron grains which subsequently influences the mode of transformation of these grains when the specimen is cooled.

Examination of specimens which had been given a heat treatment prior to the diffusion anneal showed that the grain size of the alpha iron

has an influence on the spacing of the nickel "fingers". A coarse alpha-iron grain size resulted in wider spacing between the "fingers". However, the depth of penetration as determined by metallographic examination alone was not affected. That is, although there were fewer "fingers" per unit length along the interface, their lengths were the same in the as-received and heat-treated specimens.

Autoradiographic. In Fig. 3 are shown autoradiographs of a series of diffusion specimens from radioactive nickel. The diffusion times for these specimens vary from 5 to 338 hours at a temperature of 1800°F. These autoradiographs show that grain-boundary diffusion of nickel into iron actually does occur in as short a time as 5 hours. Increasing the diffusion times increases the depth of nickel penetration, as can be seen by comparing these autoradiographs.

Autoradiographic evidence for the influence of prior heat treatment on the characteristics of nickel diffusion in iron is illustrated by Fig. 4. The wider spacing of the nickel "fingers" in the heat-treated specimen is definitely noticeable in these autoradiographs.

In all the autoradiographs of specimens diffused at 1800°F, it can be noticed that there are grain boundaries of the iron which apparently contain no nickel. Furthermore, in some cases, the nickel "fingers" extend into and stop within an iron grain. This situation results from the fact that gamma iron transforms to alpha iron when cooled to room temperature from 1800°F. The grain boundaries which appear in the autoradiographs are not necessarily the ones in which the nickel diffused.

Figure 5 is an autoradiograph showing the nature of nickel diffusion at 1800°F into an austenitic stainless-steel specimen. In this case, there are no complications due to phase transformation on cooling and it can be seen that the nickel penetration is following along the existing grain boundaries.

Only a few diffusion runs were made at temperatures in the alpha-iron region. Figures 6a and 6b are autoradiographs of a specimen diffused at 1300°F. Figure 6a, which is an autoradiograph of the etched surface, shows that the diffusion is proceeding along the grain boundaries. Autoradiographic evidence of the pattern of these penetrations of nickel can be seen more clearly in Fig. 6b, where the specimen has not been etched. Figure 6c is a conventional photomicrograph of an iron specimen plated with stable nickel and diffused under the same conditions as the radioactive specimens of Figs. 6a and 6b. The complete lack of any metallographic evidence of the grain-boundary nature of diffusion at this temperature is shown in Fig. 6c. Figure 6d is an

autoradiograph of a specimen diffused at 1150°F for 185 hours. Even at this lower temperature, it can be seen that diffusion of nickel along grain boundaries occurs to a considerable extent.

Influence of Autoradiographic Exposure Time. All the autoradiographs listed above were exposed for identical lengths of time (5 days), the selection of this particular exposure time being empirical. To determine the effect of varying the exposure time, successive autoradiographs with increasing exposure time were made of the same specimen and area shown in Fig. 3c. Exposure times of 4, 8, and 16 days were used; the resulting autoradiographs are shown in Fig. 7. In making these autoradiographs only the emulsion of the previous autoradiograph was removed; the same plastic coating was used for all three autoradiographs. A conventional photomicrograph of the bare metal surface of the autoradiographed area is also shown in Fig. 7. Comparison of the autoradiographs and the photomicrographs illustrates the ability of the autoradiographic method to detect the presence of nickel at a greater depth than the metallographic examination.

These autoradiographs show that increasing the exposure time from 4 to 8 days results in a response from nickel at a depth further from the interface, but increasing the time to 16 days seems to have no further noticeable effect. Radioactive nickel-63 is ideally suited for studies of this kind because the loss of activity during the time required to make a series of autoradiographs is negligible.

Penetration Measurements. Inspection of the autoradiographs at low magnifications (e.g., Fig. 4) shows that the depth of penetration of the nickel varies considerably from one grain boundary to another. For this reason, penetration data have to be on the basis of a weighted average of measurements on a number of "fingers".

The method finally adopted involved using a microscope with a calibrated eyepiece grid. The base line of the grid was set at the interface between the nickel and iron. On grid lines parallel with the base line, the number of "fingers" intersecting a given length of grid line was counted for each grid line until a grid line was reached which had no "fingers" intersecting it. The number of "fingers" that end between the first and second grid lines can be found by subtracting the number that intersect the second grid line from the number intersecting the first. The number ending between the second and third, third and fourth, etc., can be determined in the same way. From these data a weighted average value of the depth of nickel diffusion can be found for each diffusion time. A curve relating these values with diffusion time obtained from measurements on the radioactive series is shown in Fig. 8. In this figure is also included a curve showing the maximum penetration of the nickel, i.e., the

farthest distance from the interface at which autoradiographic evidence for the presence of nickel was detected.

Discussion of Results

The results of both the metallographic and the autoradiographic study of the diffusion of nickel into iron have shown that diffusion proceeds along the grain boundaries of the iron. High-resolution autoradiographs confirm and add to information about diffusion in this sytem obtained by conventional metallographic methods. The autoradiographs have demonstrated that nickel penetration occurs to a much greater extent than can be detected by microscopic examinations.

Considering the results of diffusion at 1800°F where gamma iron is in the stable phase, some question may arise as to the correct interpretation of the grain boundaries outlined by the presence of the nickel. The conclusion that these boundaries were the grain boundaries of the gamma iron which existed at the diffusion temperature is based on several facts:

First, a conventional photomicrograph such as Fig. 7d reveals that the appearance of the "fingers" extending into the iron from the nickel plate is different from the iron grains themselves. The concentration of nickel in these "fingers" must be high enough to stabilize the gamma phase of the iron-nickel system. This occurs at approximately 6% nickel under conditions of rapid cooling. These "fingers" are remnants of the high-temperature gamma phase and if they are examined closely, an actual grain boundary can be seen extending through the middle of each of them.

Second, the fact that these "fingers" are more widely spaced at increasing distances from the interface indicates that the boundaries into which the nickel was penetrating were migrating as the diffusion proceeded. This can only be the result of gamma-iron grain growth at the diffusion temperature.

Third, the autoradiograph of nickel diffusion into an austenitic-type stainless steel shows that these "fingers" follow the grain boundaries which are visible at room temperature. In this material, there is no phase transformation and there can be no question that the nickel is penetrating along grain boundaries that existed at the higher temperature.

An interesting observation that results from further examination of the autoradiographs is that the gamma-iron grain boundaries, as defined by the nickel penetrations do not always coincide with the alpha-iron grain boundaries. This is illustrated by the autoradiographs in Figs. 3 and 7. The usual concept of phase transformation in iron and steel assumes that the alpha grains are nucleated at the gamma grain boundaries and grow until they meet each other. Apparently this is not the complete explanation,

because in the autoradiographs referred to above alpha-iron grains can be found which have grown across and consequently include a gamma grain boundary. It may be that the high-purity iron used in these experiments behaves differently in this respect from steels.

In much the same way, the autoradiographs give very convincing visual evidence about the influence of prior heat treatment and alpha-iron grain size on the gamma-iron grain size. This effect has been observed before in carbon steels by other investigators, but it is believed that this is the first time it has been noted in high-purity iron.

The mechanism of diffusion of nickel into iron consists of an initial penetration along grain boundaries and subsequent lateral diffusion from the boundaries into the grains. The acicular appearance of the iron grains near the interface is typical of rapidly cooled iron-rich alloys of the iron-nickel system.

In discussing the penetration data, it should be pointed out that these measurements are for one given autoradiographic exposure time. Increasing or decreasing the exposure should only shift the curves up or down, but the shape and slope of the curves will probably remain the same. This effect should not be very pronounced for exposure times longer than 5 days, as the autoradiographs of Fig. 7 show.

It is believed that the autoradiographs of specimens diffused at 1300 and 1150°F are the first reported evidence of grain-boundary diffusion of nickel into iron in the alpha-phase temperature ranges. These autoradiographs are strongly convincing proofs of the value of high-resolution autoradiography as a metallurgical research tool.

The metallurgical implications of the existence of grain-boundary diffusion in the nickel-iron system in both the gamma and alpha-iron regions can be quite significant. For example, the desirability of making a complete microscopic examination in connection with any determination of the volume-diffusion coefficients is strongly indicated. Otherwise, the measured values might be only a meaningless combination of grain-boundary and volume-diffusion coefficients.

SULFIDE DISTRIBUTION IN IRON

Introduction

Metallurgists have known for many years that steel with sulfide inclusions is subject to "hot shortness". It has been suggested that the presence of a liquid sulfide film at the grain boundaries of steel in the hot-working temperature range is responsible for this phenomenon. However,

several facts do not seem to be consistent with this explanation: (1) the frequent absence of continuous films of sulfide as observed under the microscope, (2) the absence of hot shortness in some high sulfur or resulfurized steels, and (3) the limitation of hot shortness to a certain temperature range. Therefore, it was proposed to investigate further the distribution of the sulfide phase in iron, particularly with the autoradiographic techniques, so that the location of the sulfur might be determined more specifically.

In this investigation, melts containing iron and sulfur were made with and without the alloying elements of silicon, aluminum, and manganese. Specimens cut from the cast ingot were annealed at selected temperatures, followed by quenching to preserve the high-temperature microstructure. After that, autoradiographic studies were applied to individual specimens.

Experimental Procedure

Materials. Vacuum-melted iron (Ferrovac "E") in the form of 1/2-inch diameter rods supplied by the Vacuum Metals Corporation, Cambridge, Massachusetts was used in this work. Its analysis was given as 0.005% C, 0.0037% O_2, and 0.00008% N_2.

The radioactive sulfur which was used, S^{35}, had a half-life of 87.1 days, with beta radiation of 0.166 mev, and was obtained in two different forms with different levels of specific activity. The low-activity form was elemental and was produced in the nuclear reactor through the reaction S^{34} (n,γ) S^{35}. It had a specific activity of approximately 0.3 mc/gm of sulfur. The high-activity form was produced by the reaction Cl^{35} (n,p) S^{35} and had a specific activity of 3530 mc/gm. Both types were obtained from the Oak Ridge National Laboratory. The high-activity sulfur was dissolved in benzene, which had to be evaporated before the sulfide was prepared.

The aluminum, silicon, and manganese used were all chemicals of commercial purity (99+%).

Sulfide Preparation. Iron and sulfur, in the form of Ferrovac chips and lumps of sulfur containing the above isotopes, were put in a pyrex tube with their relative amounts approximately equal to their stoichiometric ratio in FeS. The capsule was evacuated and sealed and left in a furnace at about 500°C for 20 hours. The temperature was somewhat critical, inasmuch as reaction rates were excessively slow at lower temperatures and the vapor pressure became extremely high at higher temperatures. Sulfur vapor reacted completely with the iron chips during this period, forming black iron sulfide. This lump of iron sulfide was ground to powdered form, which then served as the raw material of sulfur addition in the subsequent melts.

Only a relatively small amount of the high-activity sulfur was available and it was more active than considered necessary by Towe.[1] Therefore it was diluted with the low-activity sulfur by a factor of 20 to 1. Iron sulfide was made from that combination. Before dilution, the high-activity iron sulfide had approximately 500 times as many disintegrations per unit volume per second as the low-activity iron sulfide.

Melting Practice. The capsules of iron, (see Fig. 9) had one or two holes depending on the number of alloying elements. Iron sulfide was put in one hole and the other alloying element (silicon, aluminum, or manganese), if any, in the other; thus the alloying elements had no chance to react with each other before melting. The tapered plugs were pressed into the holes.

The iron capsule was then melted in an induction furnace with the arrangement shown in Fig. 10. All the meltings were done under an argon atmosphere. Argon from the gas tank was first passed through a tube containing activated alumina to absorb water vapor, and then through a furnace with titanium chips heated to above 1800°F, which would absorb most of the residual oxygen present in the argon. From there the purified gas was admitted into the pyrex tube containing the specimen. Purging lasted for about 1 hour at a pressure slightly above atmospheric.

After purging, the power input to the coil was gradually increased to the melting point of the specimen, this temperature was held for a few minutes, and then the power was cut back slowly. A typical cycle of power input is as follows: 2 min at 7 kw, 2 min at 10 kw, 5 min at 14.5 kw, and then 4 min at 8 kw. Argon was left on for about 1-1/2 hours; by then the metal had solidified and cooled to below the oxidation temperature. It was necessary to break the alundum thimble to get the ingot metal.

Heat Treatment. The metal was heat-treated at different temperatures in the hot-working range: 850°C in the α range; 950°C in the $\gamma + \epsilon$ range; and 1050, 1200, 1300, and 1400°C in the γ + Liq. range. Specimens cut from the metal ingots were sealed in an evacuated capsule of Vycor or quartz, depending on the heat-treating temperature. They were left in the furnace at the prechosen temperature long enough to obtain the equilibrium structures. The higher the temperature, the shorter the time required to attain equilibrium. The capsule was then broken under mercury to quench the specimen.

Metallographic Specimens. Specimens mounted in bakelite were polished by the usual metallographic techniques with special emphasis on preserving the nonmetallic inclusions. It was found that "Linde-A" powder is best for rough polishing and "Gamal" is good enough for fine polishing. Since pure iron is very soft, the surface of the specimen tends to be

disturbed in polishing. A technique of alternate etching (with 2% nital) and polishing on a wheel revealed the true structure.

Autoradiography. The stripping-film method described previously was employed in this investigation. Polished specimens were first coated with a layer of plastic (2% vinylite in methyl-ethyl keytone) and baked under infrared light (about 150°F) for 1 hour. Then the stripping film was put on. The exposure time ran from 4 to 10 days for specimens with low-activity sulfur and from a few hours to 2 days for high-activity sulfur.

Results and Discussion

Resolution of Autoradiographs. As mentioned in an earlier section of this report, resolution may be denoted as the minimum spacing between the radioactive sources that can be differentiated on the autoradiograph. Figures 11 and 12 will illustrate this point.

Figure 11a is a photomicrograph of an iron sample containing 0.05% sulfur (S^{35}). It was annealed at 1300°C for 3 hours and quenched in mercury. The dark triangle at the left side of the picture was a crack, at the end of which extended a film of iron sulfide presumably lying along the austenite grain boundary of iron. It is discontinuous in two places. Figure 11b shows the autoradiograph of the same area exposed for 18 hours. It shows very distinctly the concentration of activity over the iron sulfide and the gaps in between. The smaller gap is about 10 microns across; so it can be said that the resolution of this particular autoradiograph is at least better than 10 microns.

It is also possible to define resolution as the minimum spacing of an active source between two nonactive sources so that it may be detected on an autoradiograph. The technique used in Fig. 11b was sensitive enough to associate the activity with the layer of sulfide, which was approximately 1 micron wide lying between the iron grains.

Figure 12 presents the photomicrograph and autoradiographs of a sample of 0.10% sulfur, with the same heat treatment as the one with 0.05% sulfur. As shown in Fig. 12a, three austenite grains are separated by iron sulfide. Figures 12b, c, and d are the autoradiographs with exposure times of 1/2, 18, and 50 hours respectively. The 1/2-hour exposure showed evidence of more activity above the 1-micron sulfide film than did the 50-hour exposure along the boundary where the film was not observed microscopically. Thus, it might be possible to infer that if the film were truly continuous, although of a submicroscopic width, the restricted part of the film would have to be narrower than the observable part of the film by a factor of at least 100 to 1; this autoradiographic method then permits us to conclude that if the film is continuous, it must be thinner than 0.01 micron, or 100Å.

Identification of Microconstituents. Autoradiography serves as a tool to identify radioactive constituents in a sample. A few pictures shown here will illustrate this point. Figure 13a is a photomicrograph of a sample having 0.05% sulfur and 0.10% aluminum, heat-treated at 1300°C for 3 hours and quenched in mercury. This is a typical structure of sulfide with aluminum addition. Microscopic inspection does not differentiate these small inclusions as sulfides or oxides. The latter was possible, since the aluminum-containing melts oxidized very readily. In Fig. 13b the concentration of activity can be seen over and around the beads. This constitutes a proof for the presence of sulfide.

Figure 14 is an autoradiograph of a sample of iron with 0.20% sulfur and 0.50% silicon, heat-treated at 1200°C for 15 hours and water-quenched. It was noticed that activity was over the areas with sulfides, but not over the siliceous materials.

Solubility of Sulfur in Iron. For some time it was assumed that sulfur had no solubility in iron, although many considered that theoretically some solubility should exist. Recently it was pointed out[5] by thermodynamic experiments that there is a limited amount of sulfur solubility in iron. This may be corroborated by microscopic and autoradiographic results as shown in Figs. 16a, b, and c, from melts containing only sulfur and iron. In Fig. 16a the sulfur content was 0.10% and the sulfur solubility was exceeded.

In Fig. 16b and c, 0.05% sulfur was added to the melt. In the former the sulfur contained the radioactive isotope, while in the latter only the regular sulfur was added to the iron. The two samples were mounted and polished together and the stripping film covered both. The photomicrographs were taken and developed under identical conditions. The presence of general activity in Fig. 16b must be attributed to the presence of sulfur within the iron even though a separate sulfide phase was not observed. The part of the apparent activity which has to be attributed to the background or fog may be evaluated from that observed in the companion "blank" shown in Fig. 16c.

From Fig. 16 it might be concluded that on solidification, at least 0.05% sulfur goes into solution and at 1050°C the sulfur solubility is less than 0.10%. These data, although fragmentary, are in agreement with Rosenquist's[5] data.

Microstructure. Concurrent with the development of a technique for microscopic autoradiography, it is possible to take note of some of the sulfide microstructures which may be developed by metallurgical treatments.

Figure 17a shows the as-cast structure of a sample of iron with 0.20% sulfur. Among other things, the as-cast structure depends on the

cooling rate after melting, so it is not the equilibrium structure. Figure 17b shows the structure of a sample from the same melt, heat-treated at 950°C for 50 hours and water-quenched. The sulfide lies between the austenite grains, but is definitely not continuous. The equilibrium structure at 1200°C is shown in Fig. 17c. Here the sulfide phase is still essentially at the grain corners, as in Fig. 17b; however, the dihedral angle is somewhat smaller. The sample shown in Fig. 12a was equilibrated at a still higher temperature (1300°C). In this case the dihedral angle decreased to nearly zero and the film formed a more continuous envelope between and around the austenite grains, in spite of the fact that the iron in Fig. 12 contains only 0.10% sulfur, rather than 0.20% as shown in Fig. 17. Even at 1300°C the envelope was not perfectly continuous (or was less than 100Å thick), as concluded from the autoradiographs shown in Fig. 12.

An aluminum addition to the iron markedly altered the microstructures in the annealed samples (Fig. 13), producing a bead-like structure identified autoradiographically as the sulfide.

The effect of manganese additions on the microstructure is shown in Fig. 15. As expected, the sulfide is present as a manganese-rich phase rather than as the iron sulfide. The sulfide phase remained as a solid with a "globular" structure.

Initial tests indicated that silicon also has an effect on the sulfur structure within the iron. As yet, the general pattern has not been established.

DISTRIBUTION OF BISMUTH IN COPPER

Introduction

Metallurgical interest concerning the distribution of minute amounts of bismuth in cast and recrystallized copper arises due to the severely detrimental effect that bismuth has on the mechanical properties of the copper. This effect is generally attributed to the presence of the bismuth as a very thin grain-boundary film enveloping each copper grain.

A radioactive isotope of bismuth (bismuth-210) is available which can be used to study this problem of bismuth in copper. This isotope has several characteristics which are not very desirable for high-resolution autoradiography. It has a half-life of only 4.85 days and emits 1.17-mev beta particles. As mentioned earlier in this report, when this bismuth isotope emits the beta particle, it becomes polonium-210, which is an alpha emitter (5.3 mev) with a half-life of 138 days.

In the Interim Report of February, 1953, there was included a series of contact and stripping-film autoradiographs of copper-containing radioactive bismuth. In those autoradiographs, the activity pattern obtained was all due to the alpha activity of the polonium and conclusive evidence of the beta activity of the bismuth could not be found. This left some question as to whether the autoradiograph was indicative of the true bismuth distribution. Also, some difficulties were experienced in making these autoradiographs because of porosity in the copper.

Investigation of this system has been continued in an attempt to identify and locate the beta activity of the bismuth. The melting and casting were done under a controlled atmosphere to prevent difficulties due to porosity and oxides.

Experimental Procedure

Material. Irradiated metallic bismuth available from the Atomic Energy Commission was used for the bismuth additions. The specifications of this bismuth are as follows:

Catalog No.: Bi-210-I
Specific Activity: 0.4 mc/gm
Impurities: Po^{210} (daughter activity)

No attempt was made to remove the polonium before use. However, melting and heat treatment of the bismuth-copper samples were performed within one half-life (5 days) after irradiation of the bismuth. At this point, the activity due to polonium is less than 4% of the bismuth activity.

The copper used was a vacuum-melted copper (Cuprovac) obtained from the Vacuum Metals Corporation with a purity of better than 99.99% copper.

Melting. For the purposes of radiation safety and sound metal structure, a controlled-atmosphere melting furnace (Fig. 18) was constructed. With this unit, the whole process of melting and solidification could be carried out under an argon atmosphere. The whole melting unit was placed in a ventilated hood so that any bismuth carried out by the effluent argon would not be released into the room.

For each melt 400 gm of copper were placed in the graphite crucible and melted. After the copper had been molten for about 2-1/2 minutes, the bismuth addition was made. The copper was held molten for 3 minutes longer, at which time the crucible plug was removed and the copper allowed to pour into the lower water-cooled graphite mold.

Sample Processing. Disks approximately 1/8 inch thick were cut from the cylindrical ingots by means of an abrasive cut-off wheel. Liberal quantities of coolant were used to minimize dust and the cutting sludge was collected and thrown away.

The cold-rolling of these disk samples was performed in a hand-operated rolling mill. The percentage of cold-rolling was based on the change in thickness effected by this operation. The disks were cold-rolled without prior annealing in treatment.

Annealing of the as-cast and cold-rolled samples was carried out in a hydrogen atmosphere.

Metallurgical Specimen Preparation. Small sections were cut from the appropriate disk samples and mounted in bakelite. After preliminary polishing on emery paper, the specimens were given an electropolish in a solution consisting of 70% ortho-phosphoric acid in water at 1.7 to 1.8 volts.

Contact and stripping-film autoradiographs were made of these specimens by methods described previously.

Results

Melts of copper with bismuth contents of 0, 0.01, 0.02 and 0.03% were made. These percentages are nominal based on the weight of bismuth added, but it is believed that loss during melting was negligible. No determination of bismuth segregation from top to bottom of the ingot was made, but it should not be very pronounced with the particular melting and pouring arrangement used. Moreover, all samples used for metallographic and autoradiographic studies were cut from the bottom half of the ingot.

Annealing of the as-cast samples was carried out at 1800°F for 8 hours. Annealing times and temperatures used for the cold-rolled samples were 1 hour at 800, 1100, 1400, or 1700°F.

The results of these bismuth additions and processing treatments are presented in terms of their effect on the mechanical properties, radioactivity pattern, and metallurgical structure.

Effect of Bismuth on Ductility. The addition of bismuth to copper was found to have a very detrimental effect on the ductility of copper. Without any bismuth, samples of copper could be easily cold-rolled more than 80% without cracks forming. With an addition of 0.01% cracking occurred after about 20% cold-rolling, and with 0.02 and 0.03% the copper became completely brittle.

Effect of Bismuth on Cast Macrostructure. Macroetching the disks cut from the ingots revealed the pronounced effect that bismuth additions have in increasing the columnar structure in cast copper. Photomacrographs showing this influence are presented in Fig. 19. Inasmuch as the melting and pouring conditions were practically constant for all melts, the effect shown is not the result of different cooling rates, which could produce the same effect.

As-Cast Autoradiographs and Microstructures. No observable response was found on contact autoradiographs made on metallographic plates with exposure times of 7 and 15 days. This was true even for the sample containing 0.03% bismuth.

This lack of response in contact autoradiographs was rather puzzling in view of the fact that the stripping-film autoradiographs show the presence of alpha activity of the bismuth decay product (polonium). Autoradiographs made by the stripping-film method are shown in Figs. 20, 21, and 22. It can be observed that for a bismuth content of 0.01%, an exposure time of 33 days results in an autoradiograph with a few clusters of alpha tracks barely discernible above the background fog. However, with a bismuth content of 0.03%, a noticeable pattern of alpha activity is obtained with exposure times as short as 13 days. Examination of the autoradiographs at high magnification reveals that the clusters of alpha tracks are centered over ball-shaped particles. These particles are located within the grains, as well as in the grain boundaries. In some instances the activity over grain boundaries seems to be emanating from a more elongated boundary phase. In general though, what appeared under the microscope to be a film of bismuth in the boundary between two grains and in the interstices of three grains showed no alpha activity at all. Also, no definite evidence of the beta activity of the bismuth could be found in the autoradiographs of these specimens in the as-cast condition.

Examination of the autoradiographs at low magnification showed that the alpha activity has a definite pattern. For example, Figs. 22a and 22b show a linear pattern of activity. This linear pattern was found the columnar grain zone of the specimen. The direction of linear pattern was always in the long direction of the columnar grain. In the central equi-axed grains the alpha activity showed a definite criss-cross pattern. An example of this will be shown later. In an effort to determine whether this pattern of radioactivity corresponded to any metallurgical structure within the grains, the autoradiograph was removed on a few specimens and the metal surface heavily etched. This brought out the subgrain structure illustrated in Fig. 22d. It can be seen that the subgrain pattern follows the general features of the alpha-activity pattern.

In order to ascertain that the round particles in the center of an alpha-track cluster were not an artifact caused by the electropolishing, the autoradiograph was removed from the specimen shown in Fig. 21a. The metal surface was then given a careful mechanical polish and a very light etch. The result can be seen in Fig. 22b. The round particles now appear as very small pits and even at high magnification it is impossible to determine if these pits contain a second phase.

Annealed Autoradiographs and Microstructures. The most noticeable feature about the autoradiographs of the annealed specimens was the nearly complete lack of response to activity. Comparison of the autoradiographs of copper containing 0.03% bismuth in the cast and in the annealed condition, shown in Figs. 22a and 23a respectively, demonstrates this fact. Since the exposure times are nearly the same for these two autoradiographs, this cannot account for the difference in activity.

This difference in activity must be the result of vaporization of bismuth and/or polonium during heat treatment. It should be noted here that the surface autoradiographed in all these specimens was prepared by light grinding and polishing of the original surface exposed to annealing atmosphere. No determination of the depth of bismuth vaporization was made, since too much time had elapsed in comparison with the short half-life of the bismuth before this fact was observed.

Metallographic examination showed that most of the round particles present in the center of the radioactivity in the cast specimens had disappeared on annealing. The few that were left were larger, probably a result of coalescing.

In one area of an autoradiograph of an annealed specimen an apparent beta-activity pattern of the bismuth was observed. To check this observation, a second autoradiograph was made of the same specimen and area. If the pattern had been due to beta activity, then in the second autoradiograph there should be some polonium alpha tracks resulting from the decay of the bismuth. The two successive autoradiographs are shown in Figs. 23c and 23d. It can be seen that there is no alpha activity in Fig. 23d in an area corresponding to the clusters of pseudo-beta activity in Fig. 23c. Apparently, the pseudo-beta activity pattern is an artifact.

Cold-Rolled Autoradiographs and Microstructures. Except for the fact that cracks and fissures were observed, the microstructures of the cold-rolled specimens are identical to those of the as-cast specimens. The patterns of radioactivity shown by autoradiographs are also identical. No alpha activity was observed along the cracks and fissures which occurred along grain boundaries.

Recrystallized Autoradiographs and Microstructures. Typical autoradiographs of the recrystallized specimens are shown in Figs. 24, 25, and 26. These show that the alpha activity is still centered over the round particles, which still retain their overall linear pattern, even in the specimen annealed at 1700°F. These particles show no tendency to segregate to the new recrystallized grain boundaries, for many of them are still located in the interior of the new grains.

Due to the small amount of cold-rolling that was possible in the higher bismuth series, recrystallization was not complete, even at 1100°F as Fig. 24a shows. The particular area shown in this autoradiograph was in the center equi-axed region of the ignot. The previously mentioned criss-cross pattern of alpha activity found in this region is very noticeable in the uncrystallized areas of Fig. 24a. This same area after a very strong etching is shown in Fig. 24c where a definite criss-cross subgrain pattern can be seen.

Pronounced vaporization of the bismuth must occur somewhere between 1400 and 1700°F. This is based on the observation that an autoradiograph of the 1400°F annealed specimen shows high activity, while the 1700°F specimen does not. This can be seen by comparing the activity patterns of Figs. 25 and 26. At 1700°F some of the round particles still remain but most of them show no activity.

Discussion of Results

The pronounced effect that bismuth has in promoting columnar structure in cast copper has been observed previously by Northcott[6]. This constitutes good evidence that the bismuth additions were actually taken up by the melt. It further shows that addition of a small amount of an alloying element as its radioactive isotope does not influence metallurgical reactions.

The autoradiographic results of this investigation show that it would have been much more desirable to have used higher-specific-activity bismuth. The experimental work reported in the Interim Report was done with radioactive bismuth obtained from Chalk River, Canada, which had a specific activity approximately 7.5 times the material from Oak Ridge which was used in the present investigation. The fact that no contact autoradiographs could be obtained with the lower-activity bismuth in a comparable exposure time illustrates this point well.

Positive autoradiographs identification of the bismuth beta radiation is complicated by several factors, including the short half-life and the high-energy radiation of bismuth-210 and the low specific activity of the material used in this investigation. The short half-life limits the

number of successive autoradiographs that can be made from the same specimen using a reasonable exposure time. The high energy of the beta radiation is a factor in that the sensitivity of the emulsion decreases as the energy of the radiation increases. The failure to obtain any evidence of the bismuth beta radiation in this investigation can be attributed to a combination of these factors.

In spite of the fact that the alpha-activity pattern is only an indirect indication of the distribution of bismuth in copper, several interesting conclusions can be drawn from the results of these experiments. These conclusions imply the tacit assumption that there is no actual separation of polonium from the bismuth within the copper during the melting and processing treatment. If this had occurred, then there should be a significant difference between the alpha-activity pattern obtained from a short and a long autoradiographic exposure, since the bismuth is constantly being converted to polonium by radioactive decay. Even with exposure-time ratios of three and four, no difference was observed.

The correlation between the activity pattern and the subgrain structure indicates that segregation of the bismuth occurs during solidification. Whether this bismuth exists as a separate phase or in solid solution is impossible to determine from the results of this investigation. In any event, the effect is that these segregates act as centers of electropolishing and chemical etching pits. These segregates are probably roughly spherical in shape and very small in size, since many pits have no alpha activity associated with them, while immediately adjacent to them is alpha activity without any observable pit in the center of them, as in Fig. 20b. The pits without any alpha activity may have had all the bismuth etched out of them, while the activity without pits is coming from a subsurface segregate. Since the maximum range of an alpha particle in copper is around 11 microns, the size of the segregates must be approximately of the same order of magnitude.

The reason for the lack of radioactivity over apparent bismuth phases, as observed microscopically, is not very clear. Considering the fact that activity was observed over grain boundaries in the previous preliminary experiment using higher-activity bismuth, it may be that the concentration of bismuth in the boundaries is too low to be detected autoradiographically with the lower-activity material used in this investigation.

Figures 23c and 23d, which are successive autoradiographs of identical areas on the same specimen, illustrate a very important point in connection with the interpretation of autoradiographs: they show that chemical corrosion and localized fogging can very often be mistaken for radioactivity. This is particularly true for beta-activity patterns, which generally consist of clusters of small dots. Without the control

autoradiograph, the activity pattern of Fig. 23c might have been mistakenly attributed to bismuth beta activity.

DIFFUSION OF BISMUTH IN GRAIN BOUNDARIES OF COPPER

Introduction

In the Interim Report of February, 1953, autoradiographic evidence of the diffusion of liquid bismuth along grain boundaries of copper was reported. Experimental work since that time has been concentrated primarily on the production of bicrystals of copper having various crystallographic orientation angles between them. Preliminary metallographic studies using polycrystalline copper had indicated that bismuth penetration occurred along some boundaries and not along others. Bicrystals would provide a means of studying the relation between the depth of penetration and the relative orientation of the crystals comprising the boundary.

Experimental Procedure

Material. The copper used for growing the bicrystals was vacuum-melted copper (Cuprovac) obtained from the Vacuum Metals Corporation with a purity of better than 99.99%.

The stable bismuth used was obtained from the Belmont Smelting Company and its purity was better than 99.99%.

Radioactive bismuth was obtained in the form of irradiated metallic bismuth from the Atomic Energy Commission. The specifications of this material have been listed in a previous section on the "Distribution of Bismuth in Copper".

Production of Bicrystals. A method suggested by Chalmers[7] was used to grow the bicrystals of copper. Essentially, this method involves the use of two single crystals as "seeds" and a melting arrangement where the position of the liquid-solid interface can be controlled. The charge metal is melted and fused onto the seed crystals, and then by progressive solidification crystals having the same orientations as the "seeds" are grown from the melt.

A sketch of the arrangement used is shown in Fig. 27. The essential components are a moving induction coil, a pyrex glass tube, and a graphite boat inside a graphite cylinder. The boat is open at one end to receive a water-cooled graphite block. The seed crystals are held in place against the water-cooled graphite block with a special holder also made of graphite. Argon was admitted to the Pyrex glass tube to prevent oxidation of the graphite and the copper.

Figure 28 shows a typical bicrystal grown by this method and the graphite boat that is used. The seed crystals are cylindrical in shape with one [100] axis of the crystal parallel to the longitudinal axis of the cylinder. The relative angle between the crystals is then measured as the angle formed by the other [100] axes of the crystals and will be referred to as the angle θ of the bicrystal. The cylindrical shape of the seed crystals allows them to be used repeatedly for growing bicrystals having various values of θ. The seed crystals are cut off, etched to remove the strain in the cut surface, and then set at a different angle to grow another bicrystal.

The power for melting was supplied to the induction coil by a high-frequency generator. The induction coil is held stationary during the melting period. Once the charge and a short length of the seed crystals became liquid, the induction coil was slowly moved to cause progressive solidification from the seed crystals. The movement of the coil was adjusted so that the rate of solidification was about 0.1 inch per minute.

Although no chemical analyses were made of the bicrystals grown in this manner, it is believed that contamination was very negligible.

Preparation of Diffusion Specimens. Samples about 3/8 inch square by 3/8 inch high containing the bicrystal boundary were cut from the bicrystal ingot. The cuts were made with a thin abrasive cut-off wheel of the type that is used for glass cutting. The cut surfaces were etched in acid to remove strained metal.

The diffusion was accomplished by placing a small amount of bismuth on the top of the bicrystal sample, heating to the diffusion temperature, and maintaining that temperature for the desired length of time in a hydrogen atmosphere. The direction of diffusion was parallel to the growth direction of the bicrystal.

After diffusion, the specimens were sectioned perpendicular to the diffusion interface and across the bicrystal boundary. They were then mounted in bakelite, polished, and electrolytic-polished in 70% orthophosphoric acid solution at about 1.7 volts.

Results

Some results obtained using polycrystalline and columnar-grained material during the early phases of this investigation which were not included in the Interim Report will be presented first. Figures 29a, b, and c are photomicrographs typical of the kind of evidence which formed the basis for concluding that there are preferred boundaries for the diffusion of bismuth. In Fig. 29b the suspected penetration of bismuth appears as a

more or less continuous film, whereas in Fig. 29c the bismuth seems to occur as discontinuous particles. Examination of these boundaries under a metallurgical microscope with a sensitive-tint illumination showed that the grain-boundary phases of both the continuous and discontinuous type take on a yellow coloration after etching with ammonium perfulfate. The grain boundaries which were concluded to be bismuth-free did not show this effect.

Several series of diffusion runs were made using bicrystal specimens and stable bismuth. The values obtained for the depth of bismuth penetration by microscopic measurements are given in Table I. The values do not seem to follow any consistent trend, except that there is no diffusion in grain boundaries with the angle θ less than 20° and probably there is none with an angle greater than 70°. On these specimens, it was noticed that diffusion was apparently also occurring through the vapor phase of bismuth. Penetration was observed extending in from the surface opposite to that on which the bismuth was placed. As with the liquid, this vapor-phase penetration was never observed in boundaries with θ less than 20°.

Only a few diffusion runs were made using bicrystal specimens and radioactive bismuth. The results are rather inconclusive in that boundaries which showed microscopic evidence of the presence of a continuous bismuth film did not show radioactivity. However, the autoradiographs showed response to radioactivity in boundaries where the bismuth appeared as discontinuous particles. Autoradiographs demonstrating this anomaly are shown in Fig. 30. As in the autoradiographic study of distribution of the bismuth in copper, only the alpha activity has been registered on the autoradiograph.

Discussion of Results

The results obtained so far indicate that more experimental work is necessary before a complete evaluation of the influence of crystal orientation on the rate of diffusion of liquid bismuth in copper can be made. The use of radioactive bismuth of higher specific activity would aid materially in the autoradiographic aspects of any further work done on this system.

Although the results are not complete, they do indicate the existence of a critical value of the angle θ below which the grain-boundary diffusion of bismuth in copper will not occur. This value appears to be in agreement with values observed by other investigators[8] who have studied the phenomenon of grain-boundary diffusion in metallic systems.

TABLE I

PENETRATION OF BISMUTH ALONG GRAIN BOUNDARIES OF COPPER BICRYSTALS AT 1200°F

	Depth of Penetration in Inches After Indicated Time at Temperature	
θ	12 hours	21 hours
2	none	none
10	none	none
15	none	none
20	trace	----
26	.02	----
28	.19	----
30	.106	.105
38	.07	----
45	.10	>.25
49	>.25	----
54	.10	----
60	.05	----
64	>.25	----
71	none	----

θ = angle between [100] axes of bicrystals; other [100] axes are common to the bicrystal and parallel to the diffusion direction.

DIFFUSION OF NICKEL INTO COPPER

Introduction

In view of the very satisfactory results obtained in the investigation of the diffusion of nickel into iron, it was felt that an autoradiographic study of the diffusion of nickel into copper would be worthy of consideration. The influence of relative crystal orientations could also be investigated easily, since the bicrystals of copper used in the study of the diffusion of bismuth into copper were available.

Experimental Procedure

Material. The radioactive nickel used was the same as that used in the investigation of the diffusion of nickel into iron; its specifications have been given in the section of this report dealing with that system.

The method of growing bicrystals of copper has already been discussed in the section on "The Diffusion of Bismuth in Copper".

Specimen Preparation. Thin slices approximately 1/8 inch thick were cut from the bicrystal ingots with a thin abrasive cut-off wheel. These slices were sanded smooth, etched in acid to remove the disturbed surface metal, and annealed at 1875°F for 24 hours. One surface was then lightly sanded again and electropolished.

Radioactive nickel was plated on the electropolished surface with the cell used to plate radioactive nickel on iron. The solution was the same as that used for the iron, but the current density was reduced to 6.5 milliamperes per sq cm.

The specimens were cut from the bicrystal ingots so that the diffusion direction was parallel to the growth direction.

Diffusion Anneal. The plated specimens were sealed under vacuum in Vycor glass tubes and placed in a furnace at the diffusion temperature. At the end of the diffusion anneal, the Vycor tubes were removed and air-cooled to room temperature. It was estimated that the specimens reached the diffusion temperature in 10 minutes and required about the same time to cool to room temperature after diffusion.

Results

Microscopic examination of specimens diffused at 1200°F for 120 hours failed to show any positive indication of grain-boundary diffusion. However, stripping-film autoradiographs of these specimens revealed very

clearly that grain-boundary diffusion had occurred in bicrystals with large values of θ. These autoradiographs are shown in Fig. 31, where it can be seen that little or no grain-boundary diffusion occurs for a θ of 2 or 15° but is very pronounced for a θ of 49°.

When the diffusion temperature is increased to $1700^{\circ}F$ the rates of volume and grain-boundary diffusion appear to be about equal, for no "fingers" of high nickel concentration are found in the boundary ahead of the volume diffusion. This is illustrated in Fig. 32, which is an autoradiograph of a bicrystal diffusion specimen with a θ of 45°.

The existence of certain preferred paths of grain-boundary diffusion is well demonstrated by Fig. 33. In this case, radioactive nickel was plated on a sample of polycrystalline copper. It can be seen that nickel has diffused along one boundary to an appreciable depth, but not at all in an adjacent boundary. The failure of conventional microscopic methods in detecting the presence of nickel in the boundary is shown by the photomicrograph of the same area as that of the autoradiograph.

Discussion of Results

The results, even though only of a preliminary nature, serve as a basis for concluding that grain-boundary diffusion in metals is dependent on both relative crystal orientation and temperature. Much more experimental work is necessary to determine quantitatively the effect of these influences.

HYDROGEN IN COPPER-BASE ALLOYS

Introduction

The problem of gases in metals has been of interest to foundrymen for many years. Hydrogen in copper-base alloys has been of particular interest to the brass and bronze foundrymen and in recent years it has been quite largely accepted, though not completely, as the source of many of the defects that are apparently related to variations in the atmosphere in contact with the molten metal. Test data on the 85-copper 5-tin 5-lead 5-zinc alloy offer a good example of the variations found when melts of this alloy are made under the same conditions except for the furnace atmosphere. By varying the furnace atmosphere from oxidizing to reducing, or by introducing a source of water vapor in the pouring ladle, the density may be reduced from 8.9 to 8.4; the tensile strength from 40,000 to 18,000 psi, and the elongation from 35 to 10%. Elongation may be reduced in some cases without appreciably affecting the density or the tensile strength.

Fractures of this alloy when cast as tensile or fracture test bars, or as actual castings, show variations in color and texture which can be related to the condition of the furnace atmosphere, i.e., oxidizing or reducing.

Various investigators have measured the solubility of hydrogen in liquid copper, in copper-base alloys, and also in the solid state. While the solubility shows a sharp decrease in the transition from the liquid to the solid state, an appreciable solubility does exist in the solid state. The extent of the hydrogen in the liquid metal is definitely related to the amount of oxygen present and probably to the presence of certain alloying elements.

Examination of test bars or other castings made from the copper-base melts reveals the presence in some cases of voids resulting from shrinkage or failure to feed and from gases liberated from the molten metal but trapped during solidification. These may be visible to the eye or at low magnification. Another type of defect also occurs in metals which have been gassed during melting but is revealed only after polishing and examination under a microscope. This type has been designated as fissuring, intercrystalline or boundary porosity, or microporosity and is generally found to be associated with low elongation, or low elongation and low-tensile strength. Low density seems to have a less direct relation and is more often associated with visible porosity.

Except as mentioned above, metallographic examination fails to provide any real basis for an explanation of the differences in physical properties due to melting atmospheres. One investigator has reported a difference in the shape of the lead particles in leaded copper-base alloys when the melts are made under oxidizing and reducing conditions. This observation has not been confirmed by other work.

Assuming that the observed variations in the mechanical and physical properties of the copper-base alloys are traceable to hydrogen, it was decided to use a radioactive isotope of hydrogen (tritium) and autoradiographic techniques to investigate this problem further. Tritium is a beta emitter (0.0189 mev) and has a half-life of 12.5 years.

Experimental Procedure

Material. The tritium was obtained from the Atomic Energy Commission and had the following specifications:

Catalog No.: H-3-P
Chemical Form: Gas packaged in glass ampoules
Purity: >99%
Concentration: Approximately 2.63 curies/cc at NTP

The copper-base alloys investigated were limited to alloys of copper and tin for reasons discussed later. Electrolytic copper and CP tin were used to make these alloys.

Melting. Figure 34 is a drawing of the glass-enclosed unit used for melting the alloys under a tritium atmosphere. The size and shape of the ingot and the control conditions for the actual melting, attainment of desired temperatures, introduction and dissociation of the tritium, and cooling and solidification are discussed in detail in the Interim Report of February, 1953.

The flask and the palladium foil were used only during the preliminary runs in establishing the actual liberation and presence of tritium in the melting chamber and were eliminated from all subsequent runs. Also, for the later runs, the length of the glass furnace tube was decreased to 13 inches.

The first runs were made with 160 gm of 89-copper 11-tin alloy, giving a cylindrical ingot roughly 1 inch in diameter and 2 inches long. While the bottom of the first ingots were flat, later runs were made using a crucible with a 1/4-inch tapered bottom. The 89-copper 11-tin alloy was used in preference to the alloys containing lead and zinc in order to eliminate coating of the inside surface of the furnace tube caused by the vaporization of these elements. Later, the composition of the melt was changed to 93-copper 7-tin in order to eliminate, for the most part, the alpha-plus-delta eutectoid.

The charges for melting in the tritium-atmosphere furnace were from master melts of copper and tin made in a small induction furnace. The melts were cast as rounds in graphite molds. The diameter was slightly less than 1 inch in order to allow their insertion in the graphite crucible of the tritium-atmosphere furnace; then 160-gm charges were cut from the master melt and placed in the glass melting unit along with the ampoule containing the tritium. The unit was sealed and evacuated before and during the melting-down operation; or as in the case of the final melts, the charge was melted under vacuum, allowed to solidify, remelted under vacuum, and again allowed to solidify before melting under the tritium atmosphere. The vacuum pump was run continuously during these preliminary melting and solidifying operations.

In making the actual melts under atmosphere, a melt-temperature of 2250°F was assumed. This approximate temperature was obtained by controlling the power input. A melting schedule was set up on the basis of temperature measurements made on melts not involving tritium additions.

The tritium addition for the 160-gm melt was 10 mc, except for one melt in which a 20-mc addition was made.

Results

The presence of the tritium atmosphere above the melts was demonstrated by Geiger countings made on the palladium foil placed in the glass melting unit during the first runs.

The presence of tritium in the solidified melts was demonstrated by Geiger countings made on sections cut from the ingots. The counts obtained on sections cut from the various melts were invariably well above the background count, but varied in the ratio of 1:25 for similar-size sections from melts made under supposedly similar conditions. Part of this variation may be attributed to small differences in the procedure for cutting the sections or their preparation previous to the measurement. This would imply that the hydrogen is in a rather loosely bound state, so that the hydrogen very close to the surface escape in the polishing and etching operations.

Retention of the tritium in the solidified metal was also indicated by the presence of typical intergranular microporosity or fissuring in the polished sections of the melts made under tritium, as shown in Fig. 35.

Determination of hydrogen (tritium) distribution using autoradiographic techniques was attempted on typical sections from seven melts. These melts were either 89-copper 11-tin, or 93-copper 7-tin with 10-mc tritium addition, except for one melt of 93-copper 7-tin alloy in which 20 mc of tritium were added.

The use of No-Screen x-ray film proved unsuccessful as a means of obtaining a record of tritium distribution in the polished sections. The use of Kodak metallographic plates using exposure periods ranging from 2 days to as long as 4 weeks gave a general darkening of the area of the plate directly in contact with the polished or polished and etched sample. Autoradiographs typical of the effects obtained on sections from the different melts are shown in Figs. 36, 37, and 38. Figures 36 and 37 show the darkening obtained in the actual contact areas, while Fig. 38 shows a portion of the area where direct contact was made between the metal and the plate and an adjoining area not in contact with the metal section. The latter area shows little or no darkening.

A careful microscopic examination of the darkened areas on the plates failed to reveal any well defined distribution effects which could be related to the microstructure of the cast alloys.

Use of the stripping-film technique was also employed as a means of checking the distribution of tritium, but with little or no success. Sections of metal were used in the polished and unetched and in the polished and etched conditions. Various etching solutions and different procedures for the application of the plastic protective coating prior to the placing of the emulsion were used, but no clearly defined evidence of the distribution of tritium was found, although the exposure periods were varied from 1 day to 4 weeks.

Discussion and Conclusions

The retention of hydrogen (tritium) in the solid state is confirmed for the copper-tin alloys.

The distribution of the hydrogen appears to be general. There is no evidence of grain-boundary concentration of tritium in either macro or micro grain boundaries. Neither is there evidence to indicate a low concentration at grain boundaries. There is a possibility of subgrain distribution effects.

The results obtained so far in the investigation also raise the question as to whether the same effect may be expected from an atmosphere of tritium as from one of normal hydrogen.

AUTORADIOGRAPHIC STUDIES OF SPHERULITIC GRAPHITE FORMATION IN CAST IRON

Introduction

The change in the shape of the graphite in cast iron from a flake form to spherulitic as a result of addition of cerium or magnesium to the molten metal is a well-known phenomenon and is the basis of the commercial production of cast iron with high ductility. However, up to the present time no satisfactory explanation of the mechanism by which this change in graphite shape occurs is available, nor has the location of the residual cerium or magnesium in the solidified metal been determined.

Several radioactive isotopes of cerium are available from the Atomic Energy Commission but none of magnesium. It was felt that the use of radioactive cerium and high-resolution autoradiographic techniques could aid in the solution of this problem. Further consideration along this line revealed, however, that the reduction of the cerium from its oxide, which is the chemical form of this element normally available from the Atomic Energy Commission, to the metal would be quite difficult. Also, the radioactive decay characteristics and products of cerium are not desirable from an autoradiographic standpoint.

For these reasons, it was decided to investigate the distribution of sulfur in cast iron containing spherulitic graphites, since this information would be helpful in determining the mechanism of spherulitic graphite formation.

Experimental Procedure

Material. The specifications of radioactive sulfur have already been given in the section on "Sulfide Distribution in Iron". The low-specific activity sulfur was used.

Commercial pig iron and ferro-alloys were used for these experiments. Both stable and radioactive sulfur additions were made in the form of iron sulfide.

Melting Procedure. Numerous trial runs using nonradioactive materials were made in order to determine the proper analysis, additions, and melting conditions for obtaining spherulitic graphite in small melts of cast iron (approximately 60 gm). The magnesium recovery was hard to duplicate from melt to melt. The trial runs showed that the following analysis gave the best results.

Carbon: 3.5%
Silicon: 2.5%
Manganese: 0.20%
Cerium: 0.01%
Magnesium: 0.1%
Sulfur: 0.025%

The cerium and magnesium content varied with recovery.

A charge consisting of pig iron, Armco iron, ferro-silicon, and iron sulfide was put into an alundum crucible and melted in a high-frequency induction coil. When the melt reached a temperature of 2600 - 2650°F, the innoculant, consisting of magnesium, nickel, cerium, silicon, and iron, was added. This addition was made by packing the innoculant in filter paper, wiring the paper to a quartz rod, and plunging the rod into the melt at the proper temperature. The power was then shut off and the melt allowed to solidify in the crucible.

For the radioactive heats, a transite box was built in order that the whole melting operation could be carried out within the box. The box was provided with a glass window and a covered opening for optical pyrometer measurements and insertion of the quartz rod for making the additions. An exhaust fan connected to the box carried any contaminated fumes to the outside.

Results

Geiger countings in a gas-flow counter of cast-iron specimens made with addition of radioactive sulfur and with ordinary sulfur definitely established that radioactive sulfur had been introduced. The count on the radioactive specimen was considerably above background.

A stripping-film autoradiograph of a cast-iron specimen made with radio-active-sulfur addition and containing spherulitic graphite is shown in Fig. 39. An activity pattern which could have been caused by segregation of sulfur or sulfides can be seen in this autoradiograph. However, in view of the small amount of sulfur added to the melt, this activity response seemed unusually strong. For the purpose of checking background and artifacts, a stripping film was applied on a specimen of cast iron made in an identical manner but with ordinary sulfur. The result is shown in Fig. 40, where it can be seen that an activity pattern very similar to the radioactive specimen is obtained. Evidently this is a case of artifacts due to localized chemical action at certain preferred areas.

Discussion of Results

Because of the artifacts which appear on the control specimen, it is impossible to draw any conclusions regarding sulfur distribution from the autoradiograph of the radioactive specimen. This illustrates very convincingly the need for control specimens and exposures for the proper interpretation of autoradiographic results.

The artifacts appeared in this case despite the use of a thin plastic protective layer which had proved satisfactory for the study of other metallurgical systems and problems. Sulfur is well-known as a photographic sensitizing agent and is effective in very low concentrations.

Further analysis is needed to distinguish between chemically-induced and radiation-induced patterns in the autoradiograph.

REFERENCES

1. Towe, G.C., Gomberg, H.J., and Freeman, J.W., "High-Resolution Autoradiography", NACA Tech. Report (to be published).

2. Gomberg, H.J., "A New High-Resolution System of Autoradiography", Nucleonics, 9, No. 4, 28 (1951).

3. Wells, C., and Mehl, R.F., "Rate of Diffusion of Nickel in Gamma-Iron in Low-Carbon and High-Carbon Steels", Trans. Am. Inst. Mining Metal. Eng., 145, 315-28 (1941).

4. Kuczynski, G.C., and Alexander, B.H., "A Metallographic Study of Diffusion Interfaces", Jour. App. Phys., 22, 344 (1951).

5. Rosenquist, T., and Dunicz, B.L., "Solid Solubility of Sulfur in Iron", Trans. Am. Inst. Mining Metal. Eng., 194, 604 (1952).

6. Northcott, L., "The Influence of Alloying Elements on the Crystallization of Copper. Part I Small Additions and the Effect of Atomic Structure", Journ. of Inst. of Metals, 62, 101 (1938).

7. Chalmers, B., "The Preparation of Single Crystals and Bicrystals by the Controlled Solidification of Molten Metals", Canad. Journ. of Phys., 31, 132-46 (January, 1953).

8. Flangan, R., and Smoluchowski, R., "Grain Boundary Diffusion of Zinc in Copper", Jour. of App. Phys., 23, 785-7 (1952).

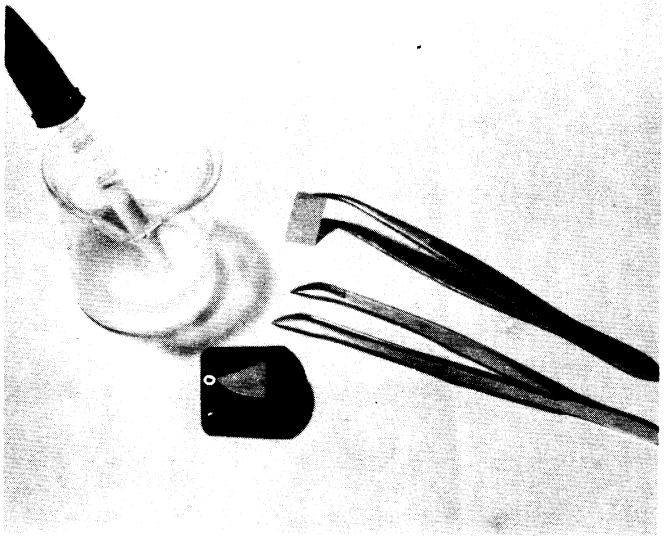

Mounted specimen ready for application of stripping film. Beaker contains water with wetting-agent addition. The film cut to proper size is shown resting against tweezer.

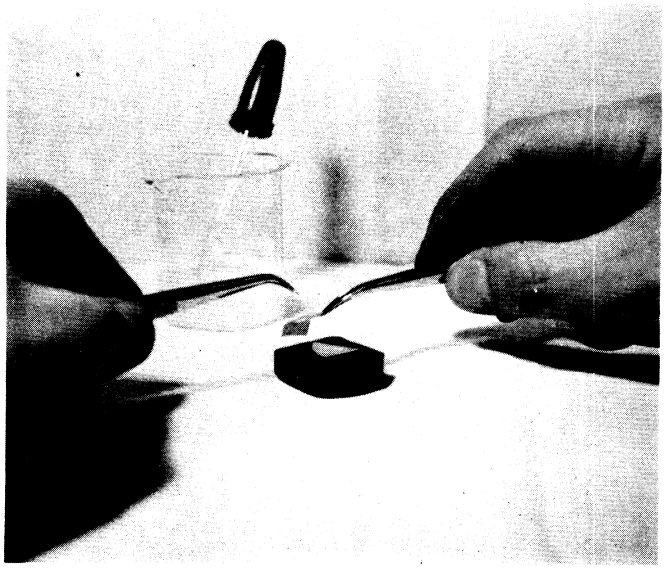

Stripping the film from the backing material with tweezers. As the film is stripped, it is laid on pool of water on the specimen surface.

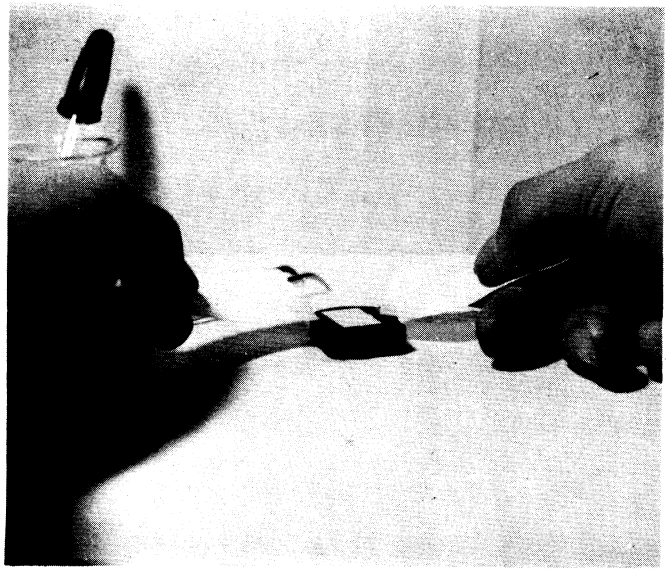

Removing the water from under the stripping film with pieces of filter paper.

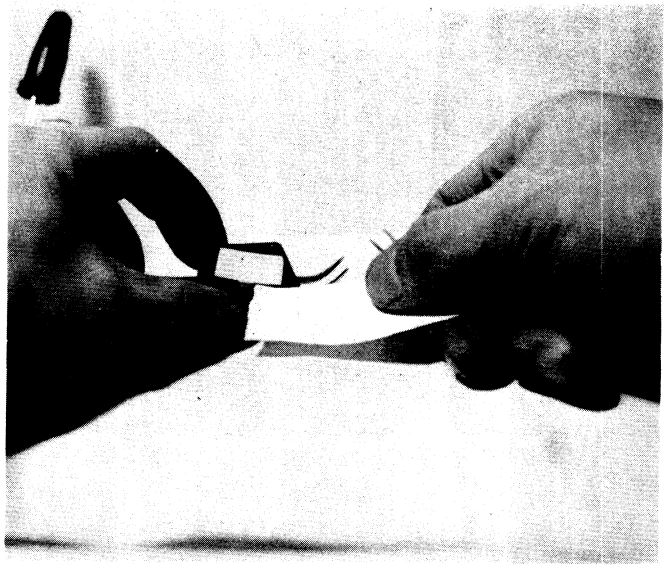

Removing last drops of water by tilting the specimen mount.

Fig. 1

Techniques of Stripping-Film Autoradiography

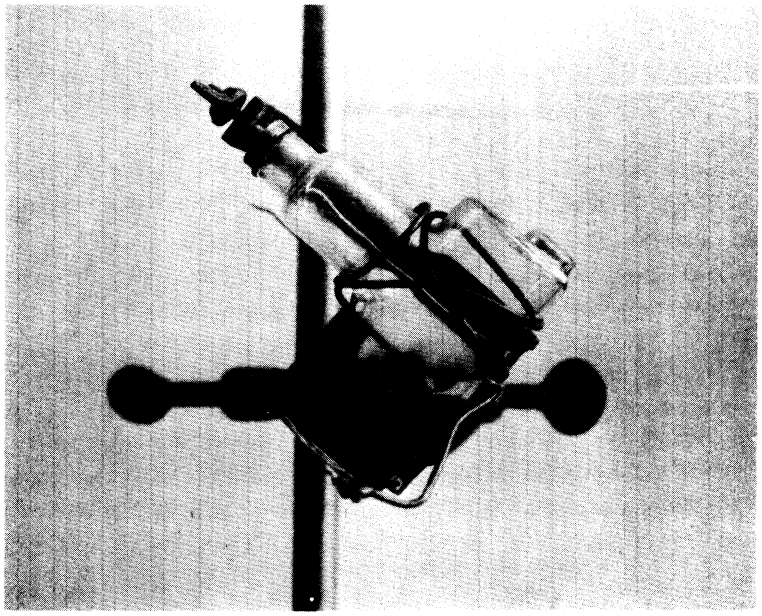

Cell in sample insertion and
removal position

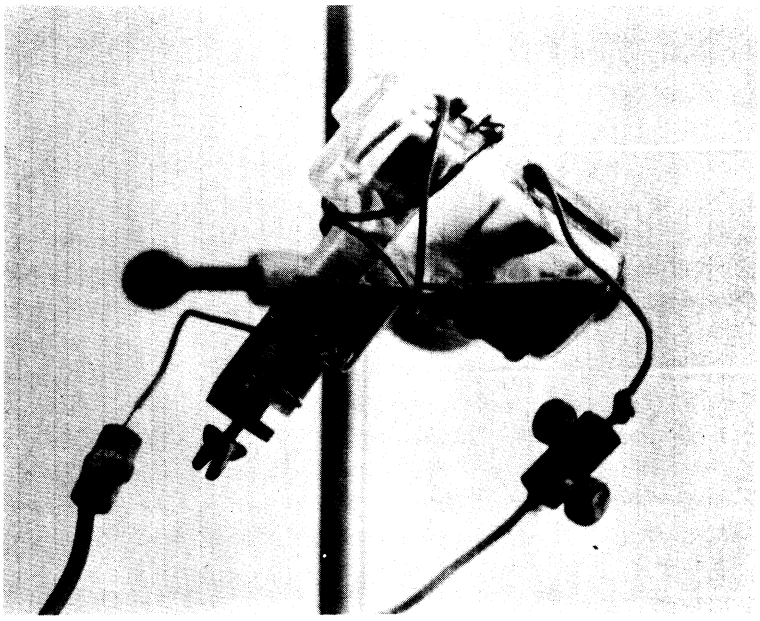

Cell in electroplating position

Fig. 2

Cell Used For Electroplating Radioactive Nickel

(a) Diffusion Time: 5 hours

(b) Diffusion Time: 42 hours

(c) Diffusion Time: 48 hours

(d) Diffusion Time: 96 hours

Fig. 3

Grain-Boundary Diffusion of Nickel into Gamma Iron
Stripping-Film Autoradiographs 500X
Diffusion Temp.: 1800°F
Sample Stock: Ferrovac Iron, as-received
Autoradiographic Exposure Time: 5 days

(e) Diffusion Time: 118 hours

(f) Diffusion Time: 200 hours

(g) Diffusion Time: 240 hours

(h) Diffusion Time: 338 hours

Fig. 3 (concluded)

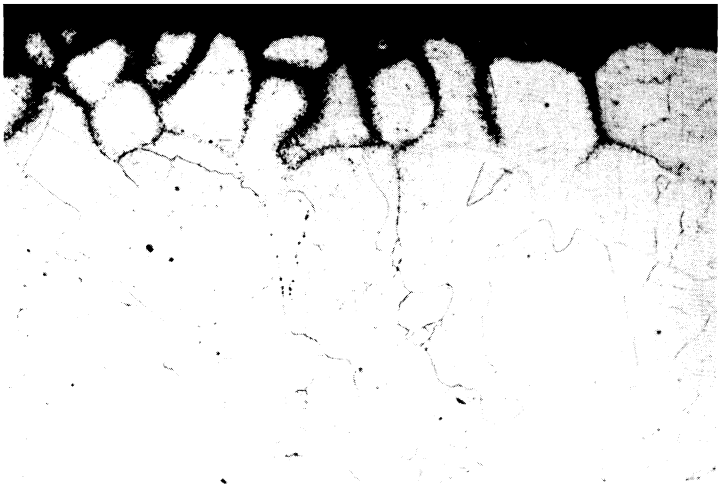

(a) As-received

(b) Vacuum-annealed, 20 hrs. at 2000° F, and furnace-cooled.

Fig. 4

Influence of Prior Heat Treatment On the Grain-Boundary Diffusion of Nickel into Iron

Stripping-Film Autoradiograph 150X

Diffusion Temp.: 1800°F
Diffusion Time: 118 hours
Autorad.Exp.Time: 5 days

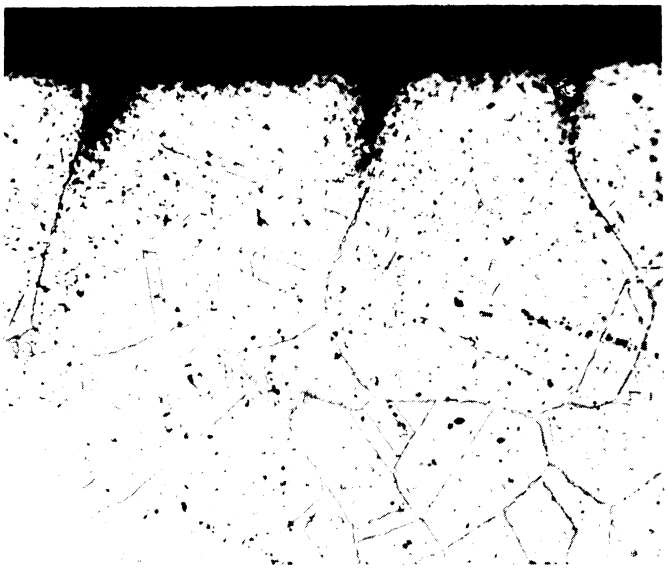

Fig. 5

Grain-Boundary Diffusion of Nickel into Austenitic Stainless Steel

Stripping-Film Autoradiograph 500X

Diffusion Temp.: 1800°F
Diffusion Time: 25 hours
Stock: 20 Ni, 24Cr Stainless
Autorad.Exp.Time: 5 days

(a) Diffused 220 hours at 1300°F
Autoradiograph of etched metal surface

(b) Diffused 220 hours at 1300°F
Autoradiograph of unetched metal surface

(c) Diffused 220 hours at 1300°F
Phtomicrograph of etched metal surface

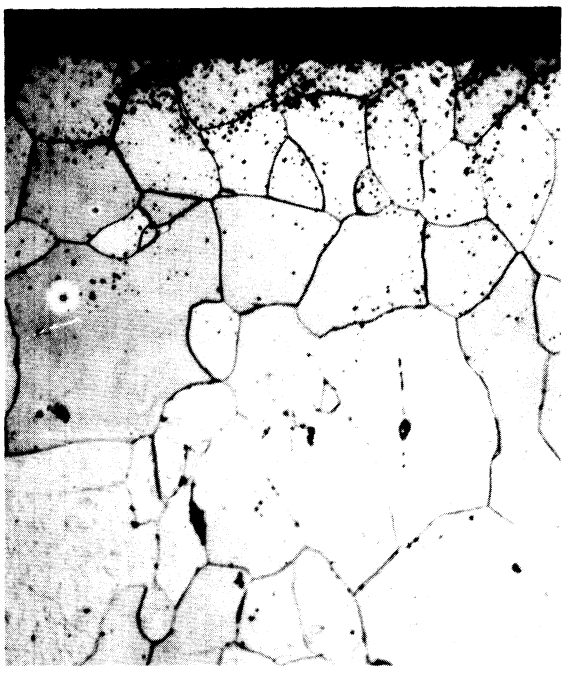

(d) Diffused 185 hours at 1150°F
Autoradiograph of etched metal surface

Fig. 6
Grain-Boundary Diffusion of Nickel into Alpha Iron

Stripping-Film Autoradiographs and Photomicrographs 500X
Diffusion Temp. and Time as indicated
Specimen Stock: Ferrovac Iron, as-received
Autorad.Exp.Time: 5 days

(a) Exp. Time: 4 days

(b) Exp. Time: 8 days

(c) Exp. Time: 16 days

(d) Photomicrograph of bare metal

Fig. 7

Influence of Exposure Time on Stripping-Film Autoradiographs of Nickel Diffusion into Iron 500X
(Specimen and area shown are same as in Fig. 3c)

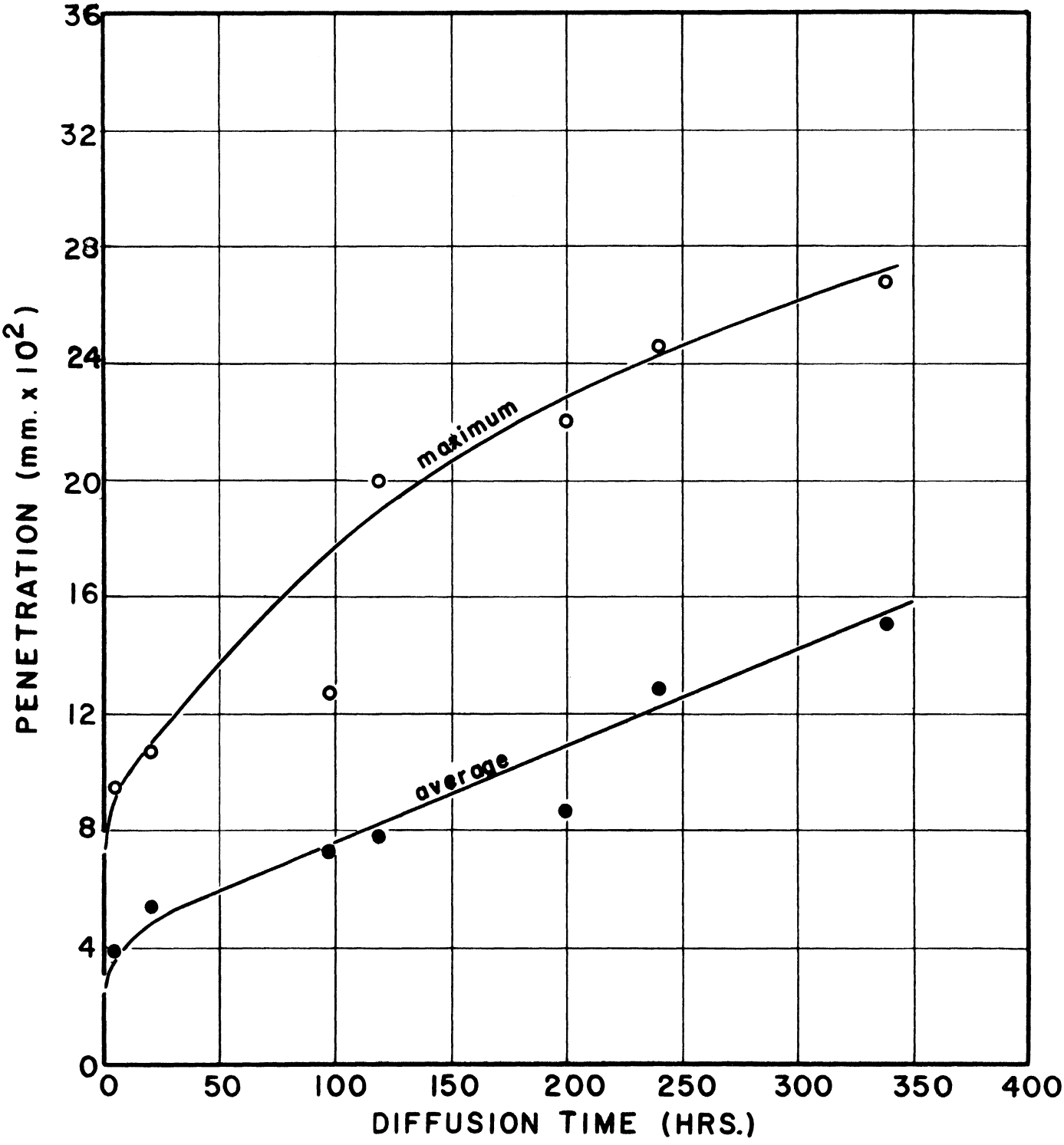

FIG. 8

MAXIMUM AND AVERAGE PENETRATION OF NICKEL ALONG GRAIN BOUNDARIES OF IRON AT 1800° F

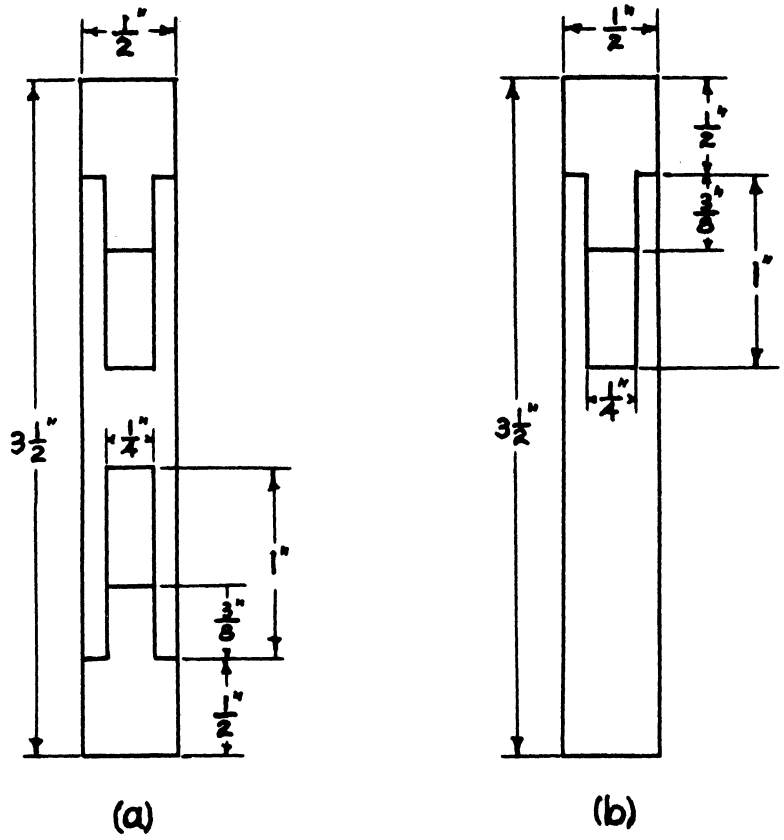

SCALE 1"=1"

Fig. 9 Capsules for Adding Sulphur and Alloys to Iron

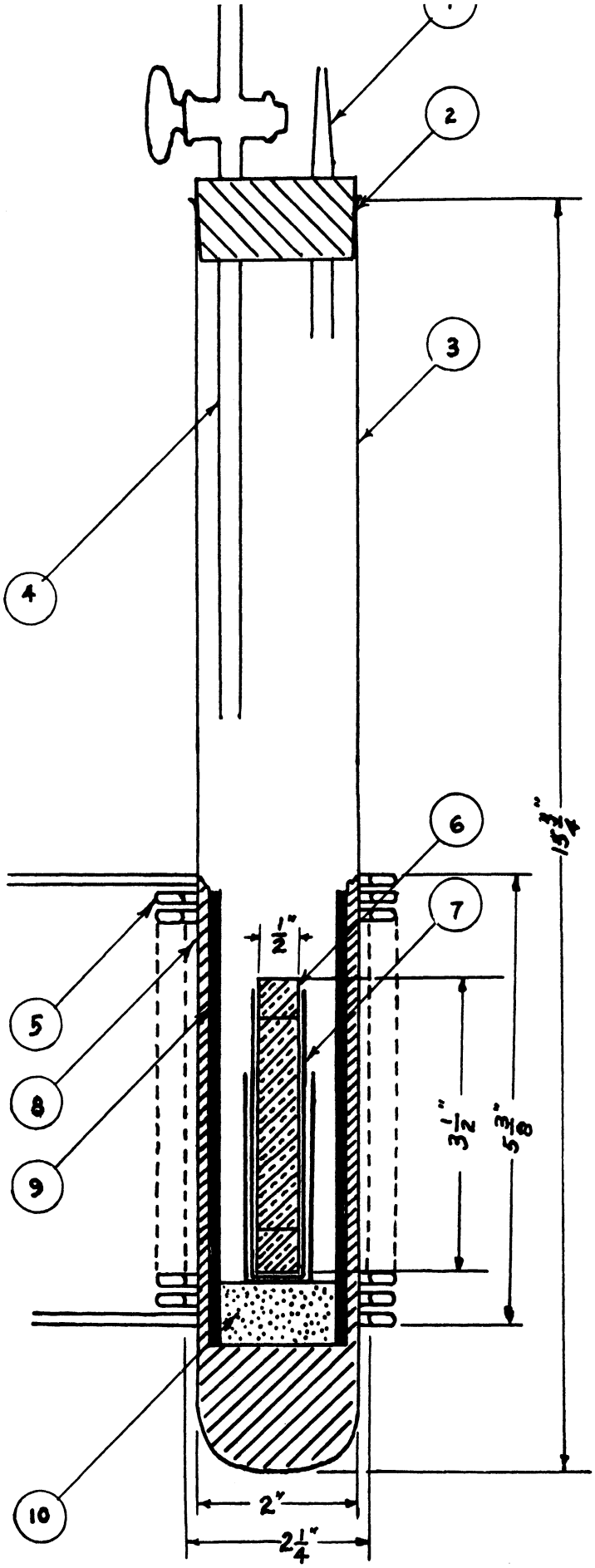

KEY TO FIGURE

1. Gas outlet
2. Rubber stopper
3. Pyrex tube
4. Gas inlet
5. Induction coil
6. Specimen (Iron Capsule)
7. Alumdum thimbles
8. Fiberfrax
9. Porcelain sleeve
10. Firebrick

Scale: 1/2 inch - 1 inch

Fig. 10

Furnace Arrangement for Melting Iron Alloys

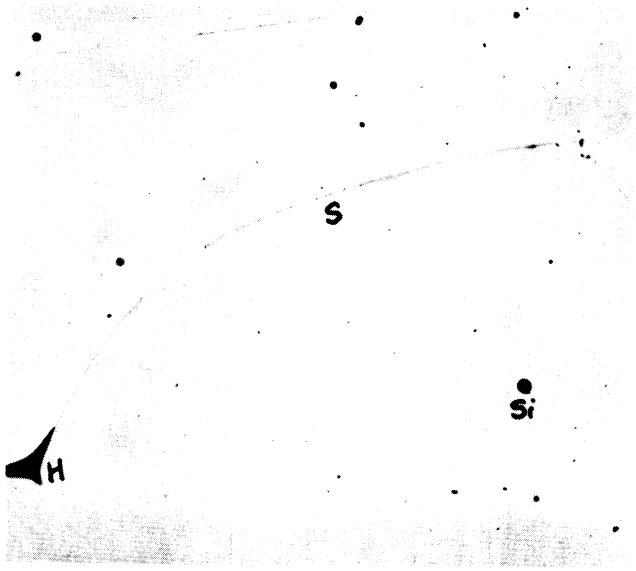

(a) Photomicrograph 250X (1 μ=0.25 mm.)

(b) Autoradiograph 250X (18-hr. Exposure)

Fig. 11

Sulphide Film between Austenite Grains.
Iron with 0.05% sulphur (high activity), annealed 3 hrs. at 1300°C, mercury quench.

S - sulphide film
Si - silicious inclusion
H - hole in specimen
C - corrosion spot

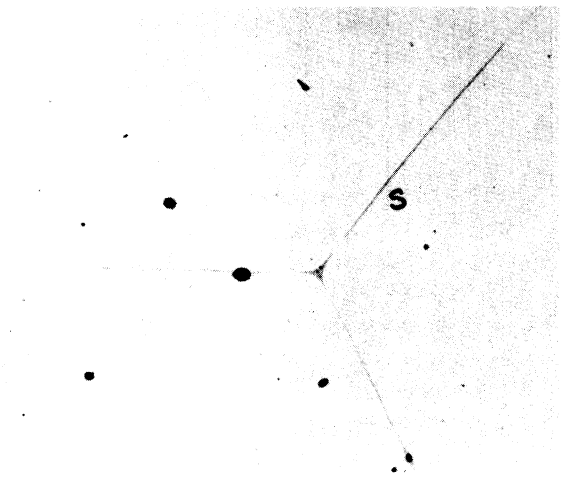

(a) Photomicrograph 250X

(b) Autoradiograph 250X
($\frac{1}{2}$-hr. Exposure)
Repolished

(c) Autoradiograph 250X
(18-hr. Exposure)
Repolished

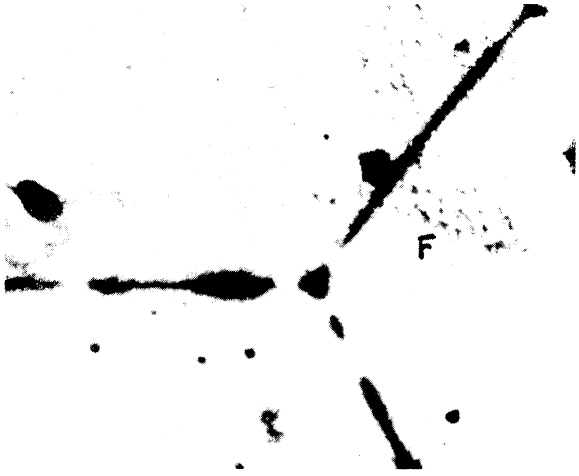

(d) Autoradiograph 250X
(50-hr. Exposure)
Repolished

Fig. 12
Grain-Boundary Distribution of Sulphide.
Iron with 0.10% sulphur (high activity), annealed 3 hrs.
at 1300°C, mercury quench.

S - sulphide,
Sh - shift of stripping film (about 4 μ),
F - fog,
C - corrosion spot.

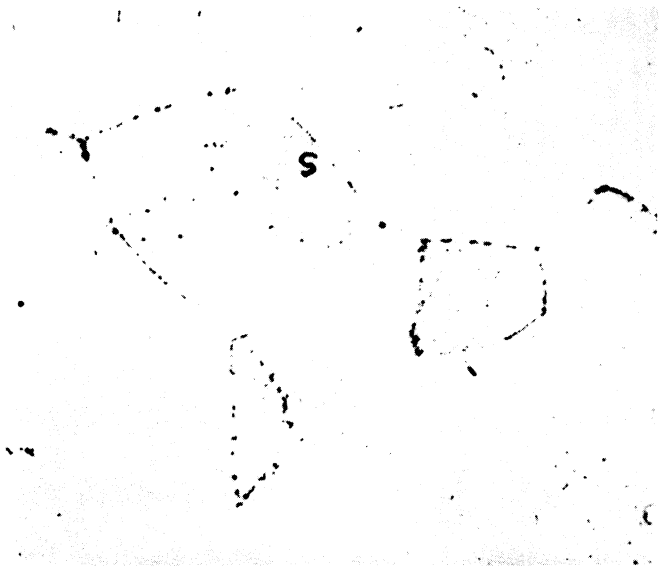

(a) Photomicrograph 250X

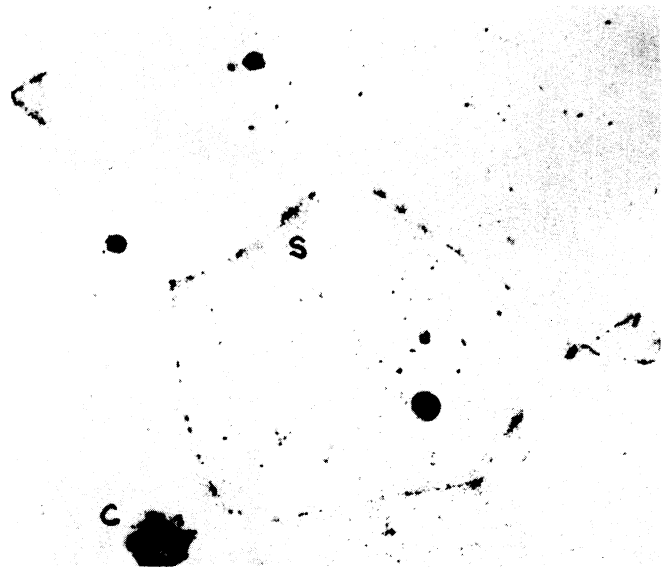

(b) Autoradiograph 250X
(18-hr. exposure)

Fig. 13 Sulphide Identification in Fe-Al-S Alloy.
Iron with 0.10% aluminum and 0.05% sulphur (high activity), annealed 3 hours at 1300°C, mercury quench.

S - sulphide "beads", C - corrosion spots

Fig. 14 Sulphide Identification in Fe-Si-S Alloy.
Iron with 0.50% silicon and 0.20% sulphur (low activity), annealed 15 hrs. at 1200°C, water quench.
Autoradiograph 500X (10-day exp.)

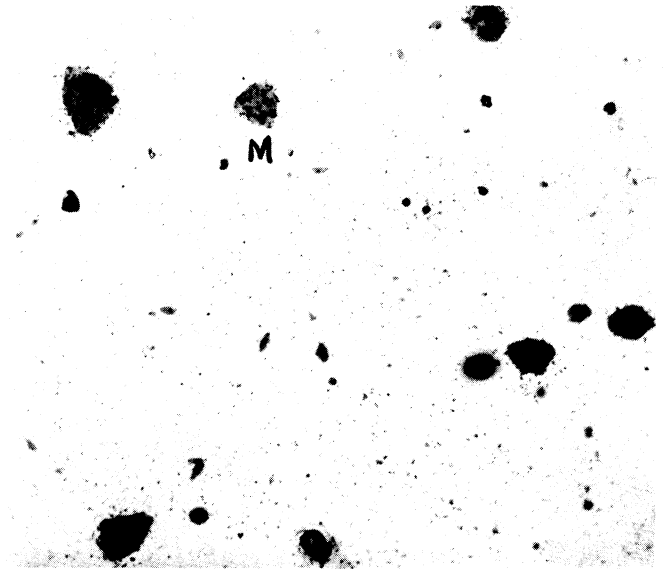

Fig. 15 Effect of Manganese on the Sulphide Microstructure.
Iron with 0.50% manganese and 0.20% sulphur(low activity), annealed 50 hrs. at 950°C, water quench.
Autoradiograph 500X (4-day exp.)

S - sulphide,
Si - siliceous inclusions
M - manganese-rich sulphide

(a) Autoradiograph 250X (46-hr.exp.)
Iron with 0.10% S (high activity)
annealed 30 hours at 1050°C.

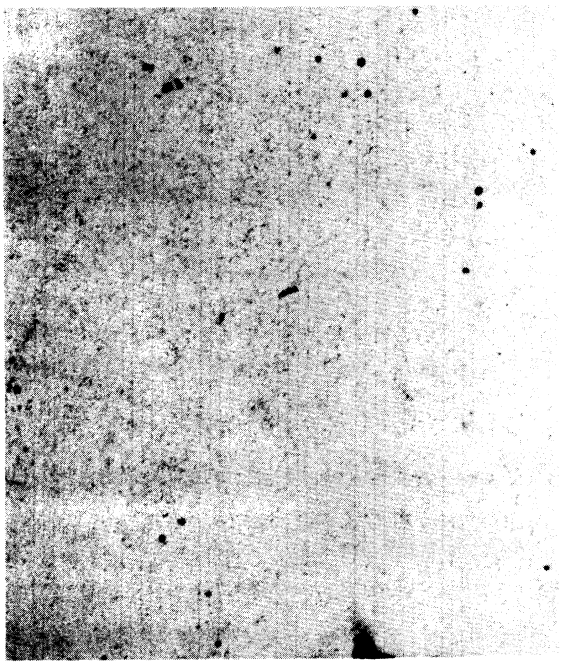

(b) Autoradiograph 250X (5-hr.exp.)
Iron with 0.05% S (high activity)
as-cast.

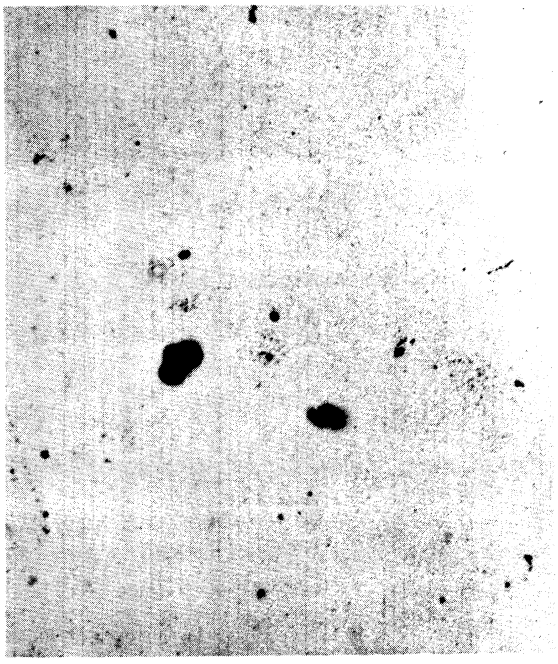

(c) Autoradiograph 250 X (5 hr.exp.)
Iron with 0.05% S (no activity),
as-cast.

Fig. 16 Solubility of Sulphur in Iron Shown Autoradiographically

(a) Autoradiograph 250X (6-day exp.)
as-cast microstructure

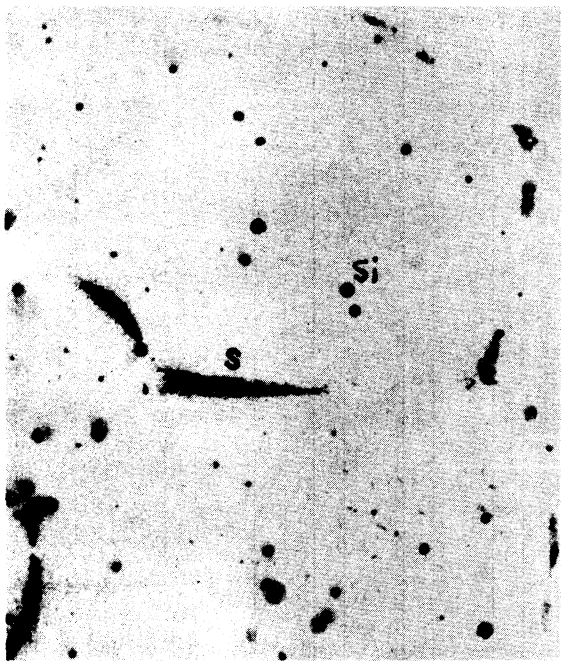

(b) Autoradiograph 250X (4-day exp.)
annealed 50 hours at 950°C,
water quench.

(c) Autoradiograph 250X (4-day exp.)
annealed 15 hours at 1200°C,
water quench.

Fig. 17 Effect of Heat Treatments on the Microstructure of Iron Sulphide.
Iron with 0.20% sulphur (low activity)

S - sulphide, Si - siliceous inclusion, C - corrosion spots

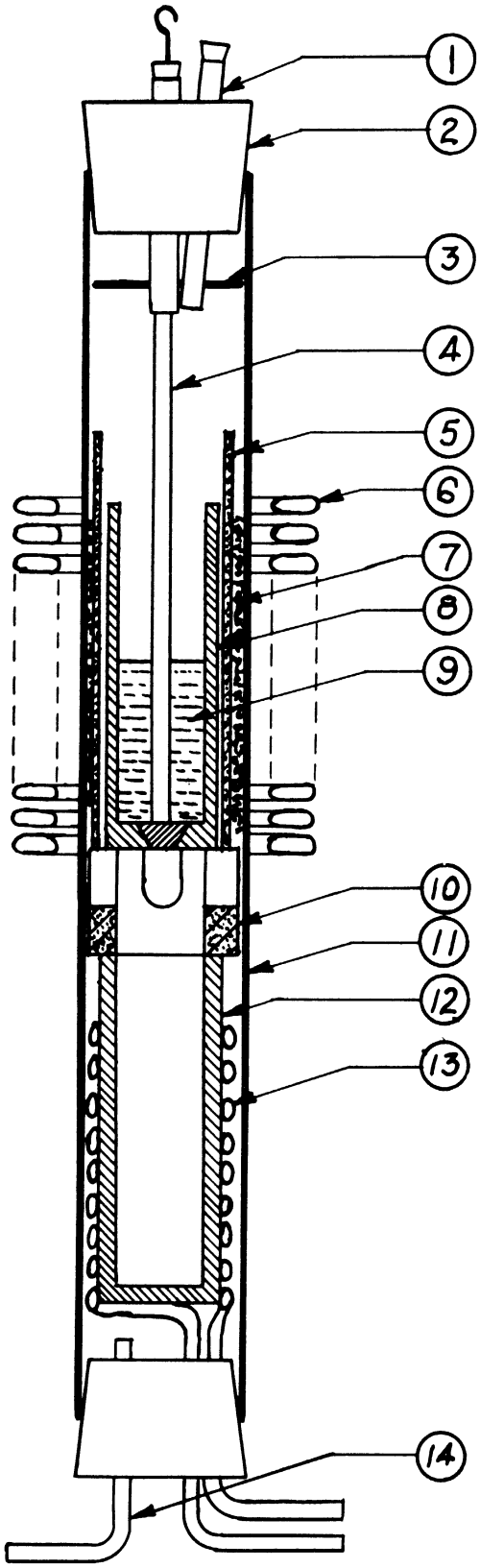

KEY TO FIGURE

1. Tube for making bismuth additions
2. Rubber stopper
3. Radiation shield
4. Graphite plug and rod
5. Ceramic cylinder
6. Induction coils
7. Fiberfrax insulation
8. Graphite crucible
9. Copper charge, 400 gm
10. Ceramic spacer
11. Pyrex glass tube
12. Graphite mold
13. Water-cooling coils
14. Argon inlet

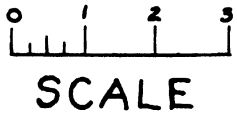

Fig. 18

Controlled Atmosphere Furnace Used for Melting Copper-Bismuth Alloys

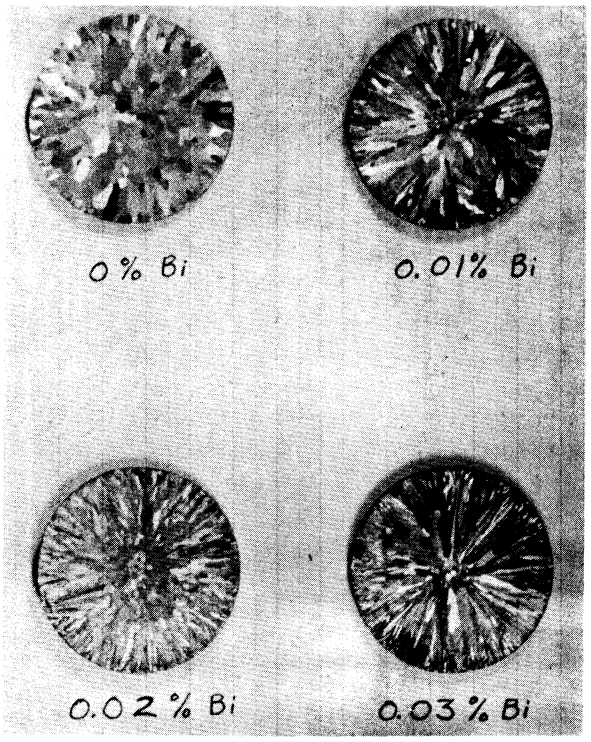

Fig. 19
Effect of Bismuth Additions on the Cast Structure of Copper

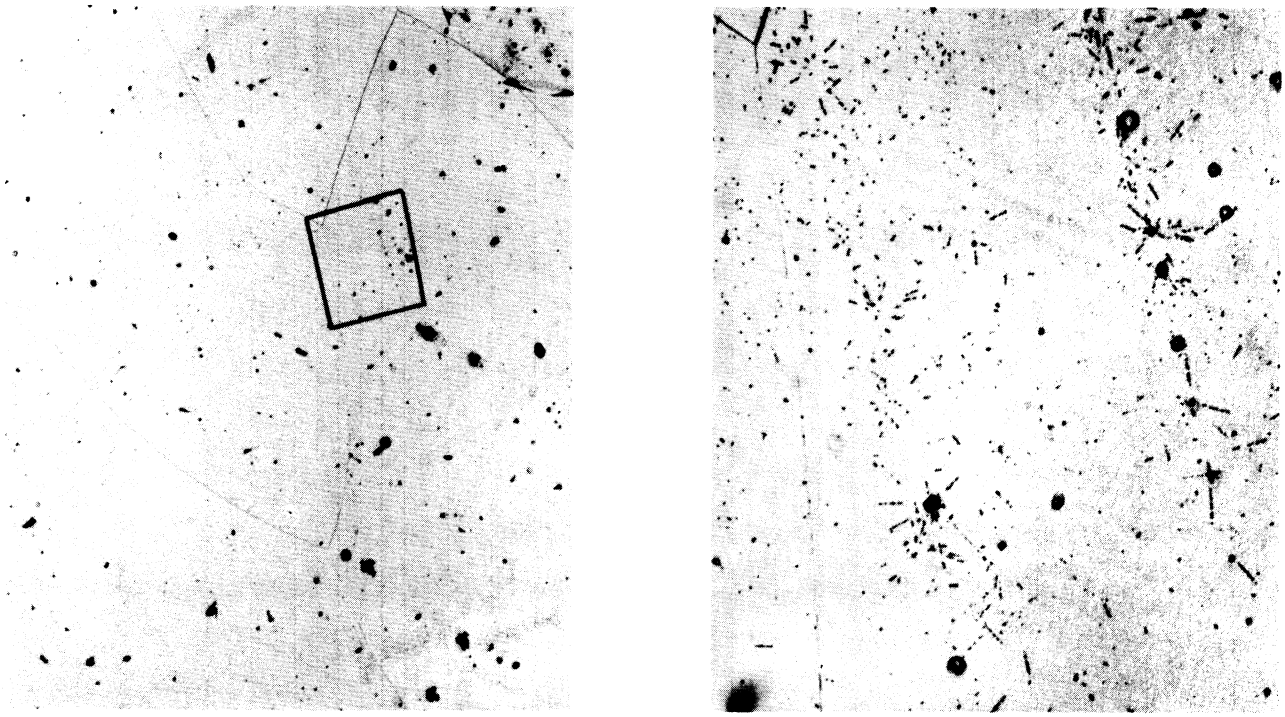

(a) 75X

(b) 500X of area marked in (a)

Fig. 20
Radioactivity Pattern of Cast Copper Containing 0.01% Bismuth

Stripping-Film Autoradiograph Expos.Time: 33 days

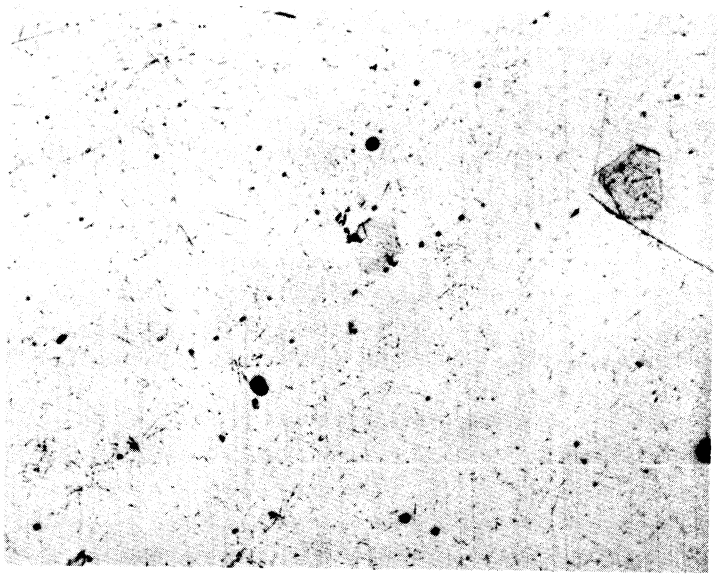

(a) Stripping-Film Autoradiograph 250X
Expos.Time:33 days

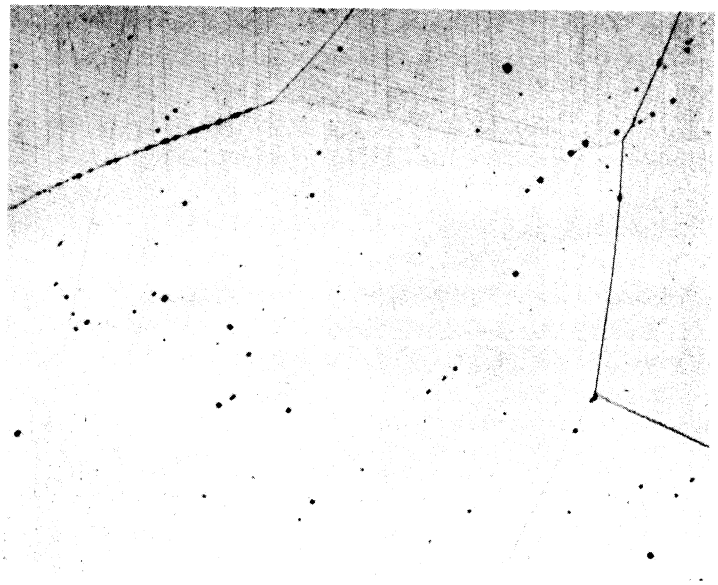

(b) Area in (a) after a mechanical polish and light etch with 20% ammonium persulfate

Photomicrograph 250X

Fig. 21

Radioactivity Pattern and Metallographic Structure of Cast Copper Containing 0.02% Bismuth

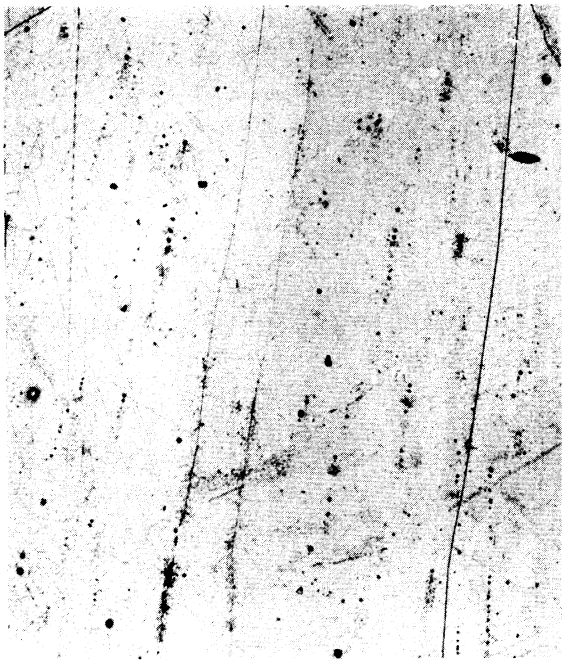

(a) Stripping-Film Autoradiograph
75X
Expos.Time: 13 days

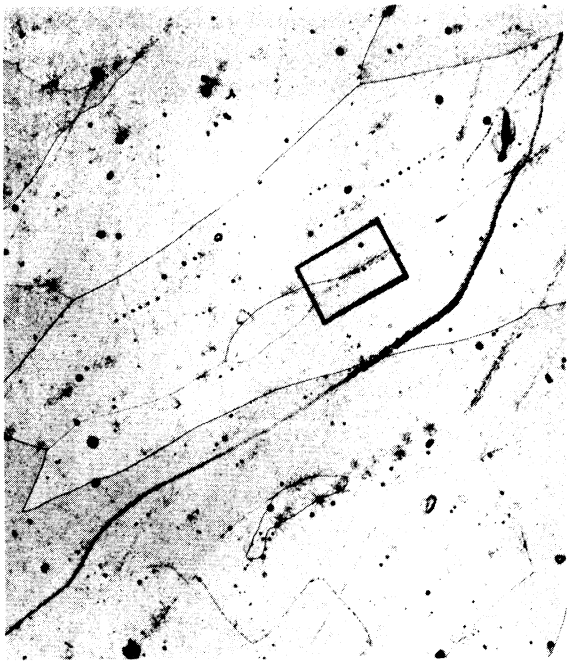

(b) Stripping-Film Autoradiograph
75X
Expos.Time: 33 days

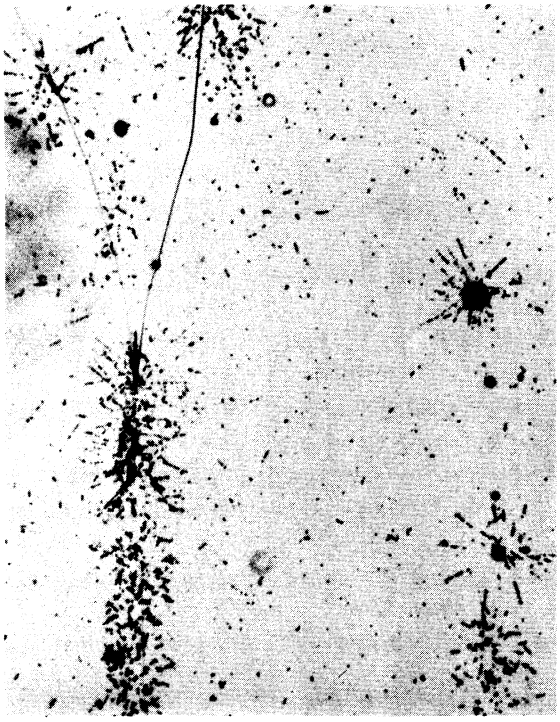

(c) Area marked in (b) at 500X

(d) Same field as (b) after deep etching with 20% ammonium persulfate to show sub-grain structure.
Photomicrograph 75X

Fig. 22
Radioactivity Pattern and Metallographic Structure
of Cast Copper Containing 0.03% Bismuth

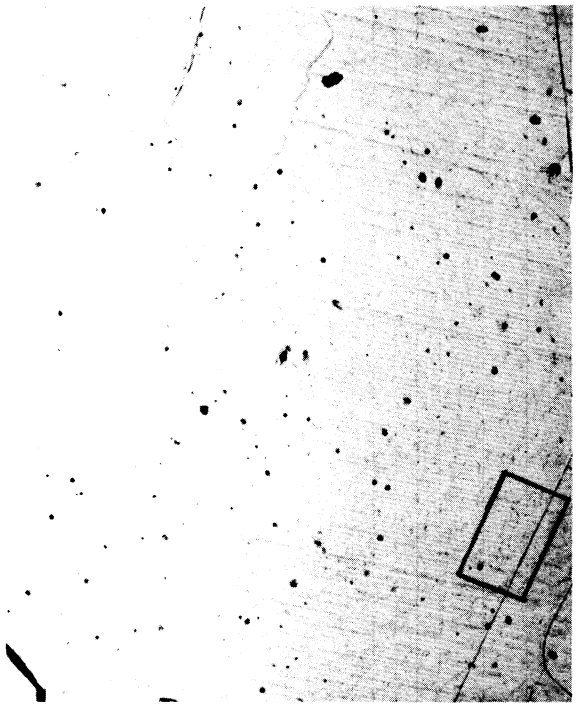

(a) Stripping-Film Autoradiograph
75X
Expos.Time: 14 days

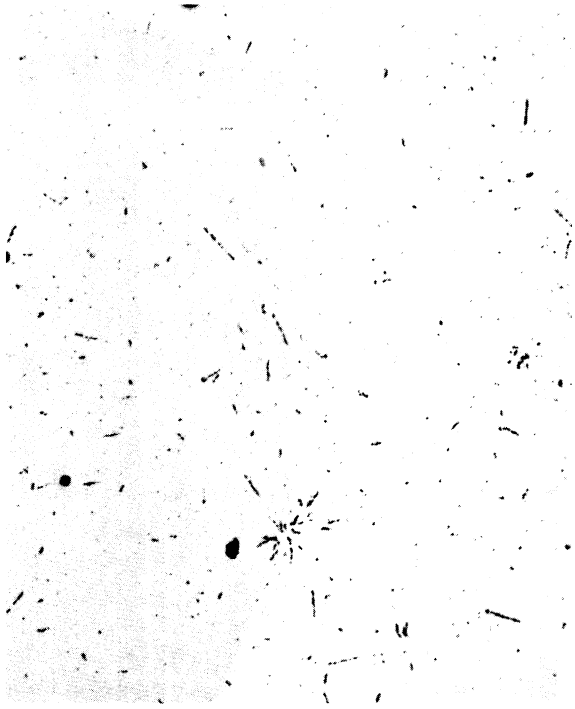

(b) Area marked in (a) at
500X

(c) Stripping-Film Autoradiograph
250X
Expos.Time: 7 days

(d) Second autoradiograph over same field as (c) and exposed for 14 succeeding days.

Fig. 23
Radioactivity Pattern of Copper Containing 0.03% Bismuth
Annealed 8 hours at 1800°F.

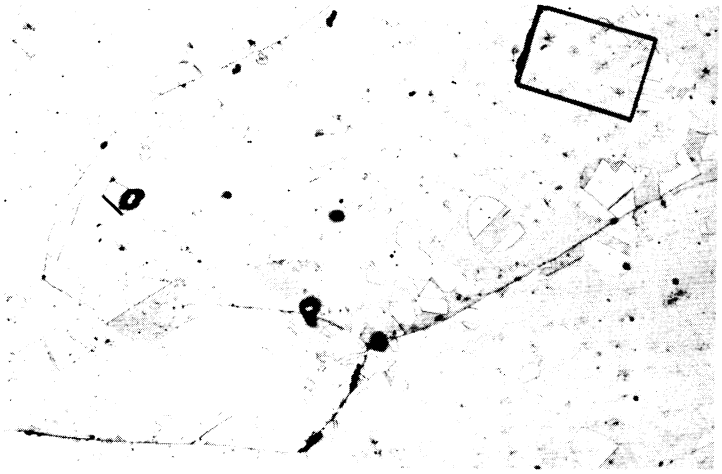

(a) Stripping-Film Autoradiograph
75X
Expos.Time: 42 days

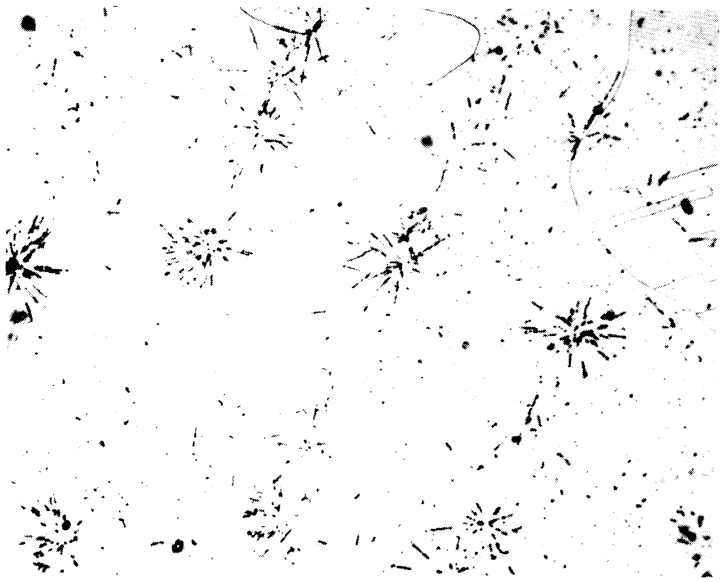

(b) Area marked in (a) at 500X

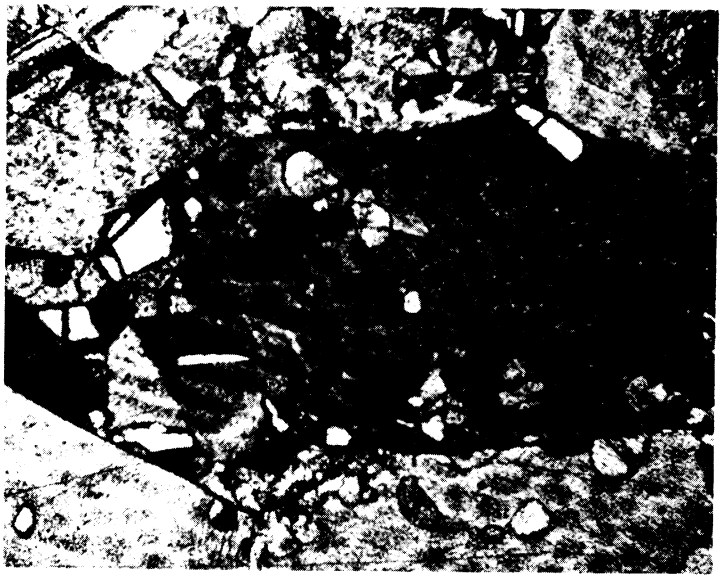

(c) Same field as (a) after deep etching with 20% ammonium persulfate to show sub-grain structure.

Photomicrograph
75X

Fig. 24
Radioactivity Pattern and Metallographic Structure of Copper Containing 0.02% Bismuth Cold-Rolled and Annealed 1 hour at 1100°F.

(a) Stripping-Film Autoradiograph 75X
Expos. Time: 12 days

(b) Area marked in (a) at 500X

Fig. 25
Radioactivity Pattern of Copper Containing 0.03% Bismuth Cold-Rolled and Annealed 1 Hour at 1400°F.

(a) Stripping-Film Autoradiograph 75X
Expos.Time:34 days

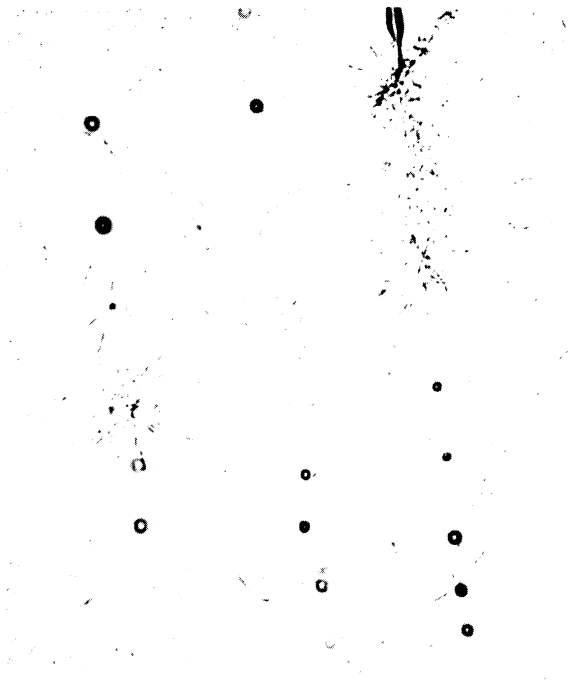

(b) Area marked in (a) at 500X

Fig. 26

Radioactivity Pattern of Copper Containing 0.03% Bismuth Cold-Rolled and Annealed 1 Hour at 1700°F.

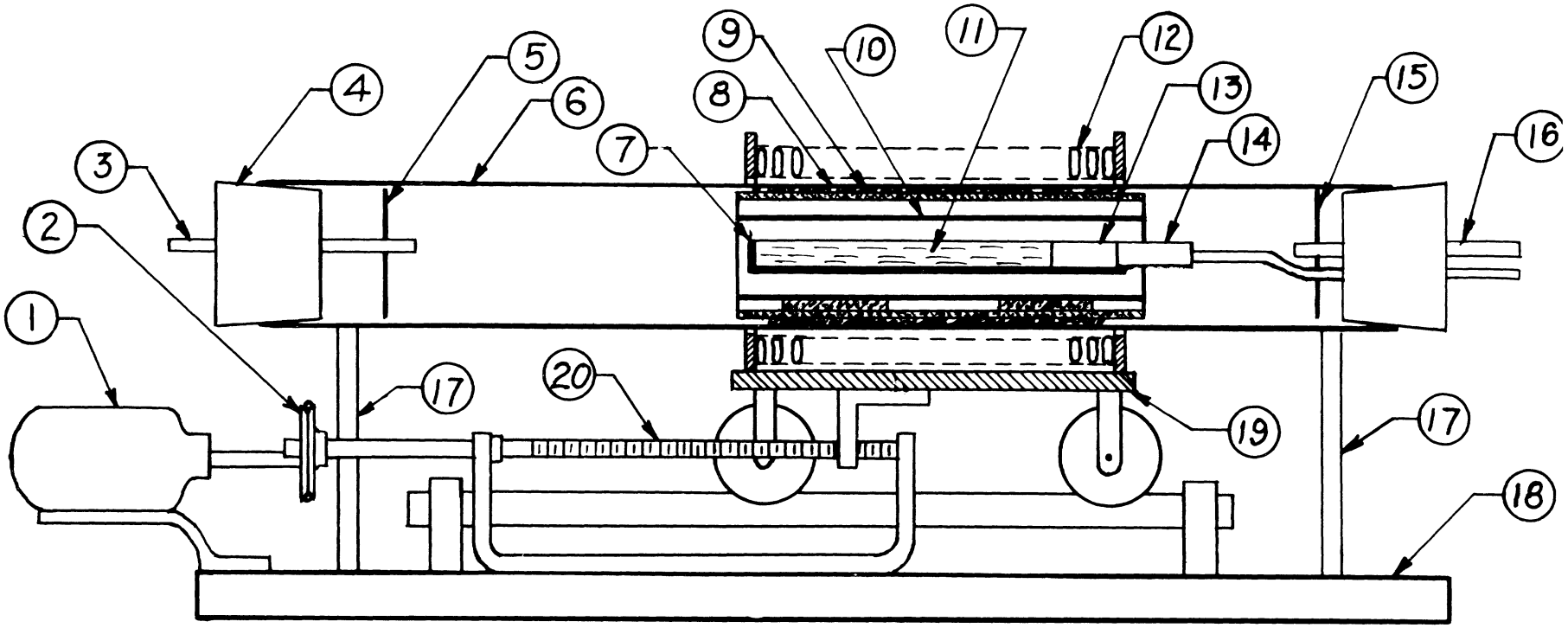

KEY TO FIGURE

1. Drive motor
2. Speed-reduction pulley
3. Argon exit
4. Rubber stopper
5. Radiation shield
6. Pyrex glass tube
7. Graphite boat
8. Fiberfrax insulation
9. Ceramic cylinder
10. Graphite cylinder
11. Copper charge
12. Induction coil
13. Seed crystal holder
14. Water-cooled graphite block
15. Radiation shield
16. Argon inlet
17. Pyrex tube supports
18. Baseboard
19. Traveling carriage
20. Drive screw

Fig. 27

Melting Unit and Drive Mechanism for Growing Copper Bicrystals

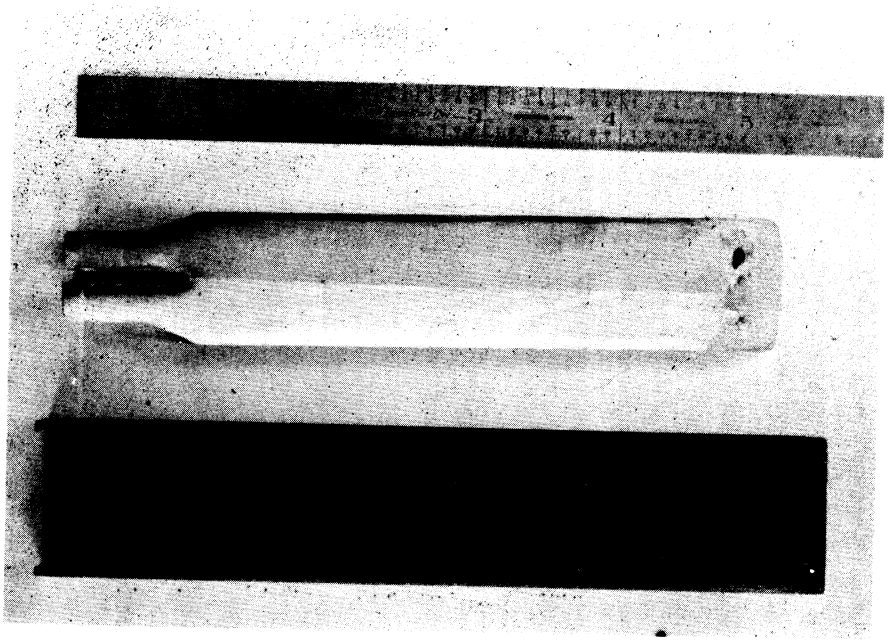

Fig. 28

Bicrystal Ingot and Graphite Boat Used
To Grow Bicrystals

(a) No penetration of Bismuth

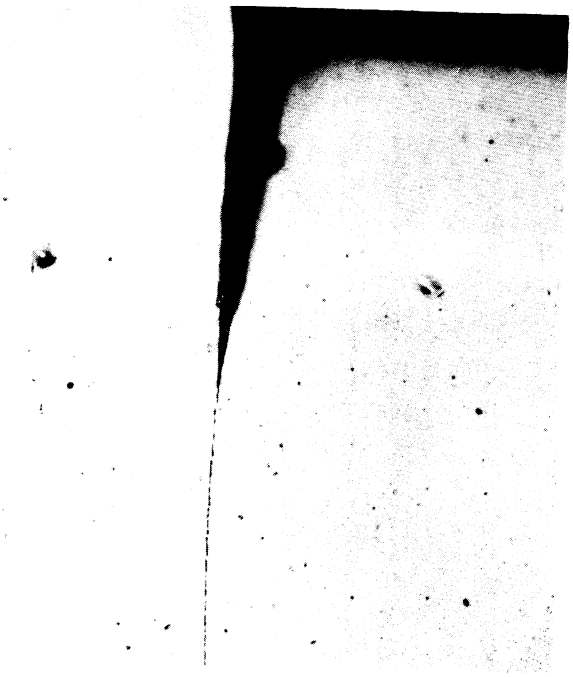

(b) Continuous film

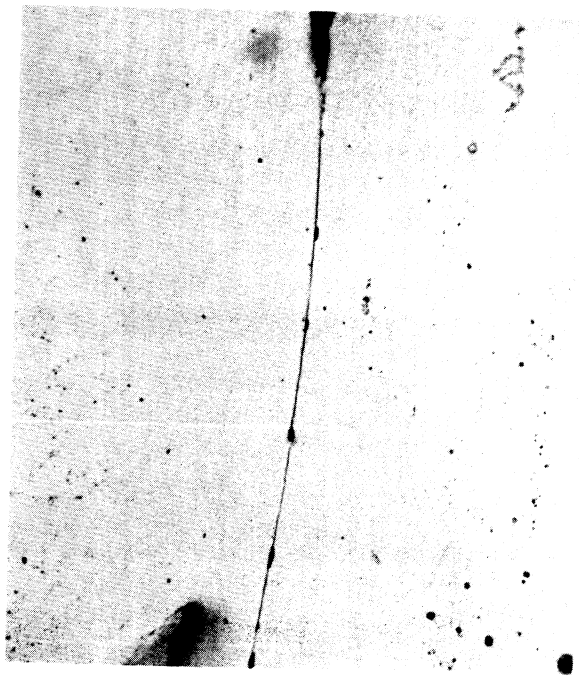

(c) Discontinuous beads

Fig. 29

Nature of Diffusion of Bismuth Along Grain Boundaries of Polycrystalline Copper at 1200°F

Photomicrograph 500X

(a) Grain Boundary Apparently Containing Bismuth
but Showing No Autoradiographic Response
Autorad.Expos.Time: 14 days

(b) Grain Boundary Showing Autoradiographic
Evidence for Presence of Polonium
Autorad. Expos.Time: 14 days

Fig. 30
Variations In Autoradiographic Response to Radioactive
Bismuth Diffused Into Copper-Bicrystal Grain Boundaries
Stripping-Film Autoradiograph
500X

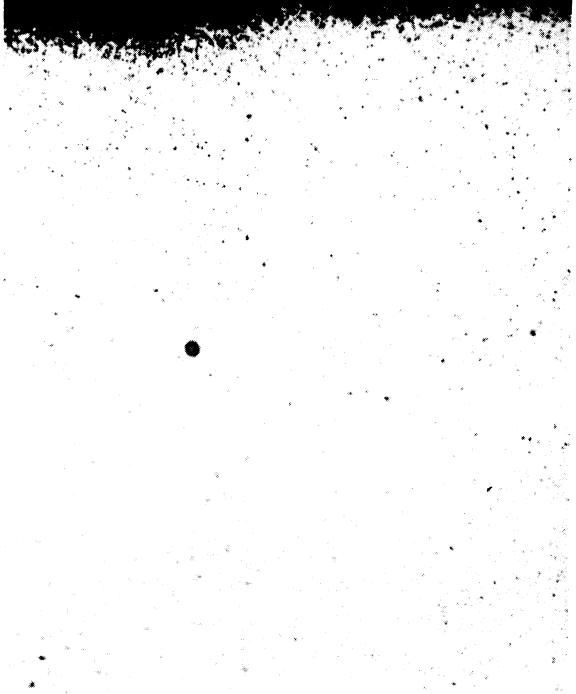

(a) $\Theta = 2^{o}$

(b) $\Theta = 15^{o}$

(c) $\Theta = 49^{o}$

Fig. 31

Influence of Relative Crystal Orientation On The Diffusion Of Nickel Along Grain Boundaries of Copper Bicrystals at $1200^{o}F$
(Θ = angle between [100] axes of the bicrystal)
Stripping-Film Autoradiographs 500X
Diffusion Time: 120 hrs.
Autorad.Expos.Time: 5 days

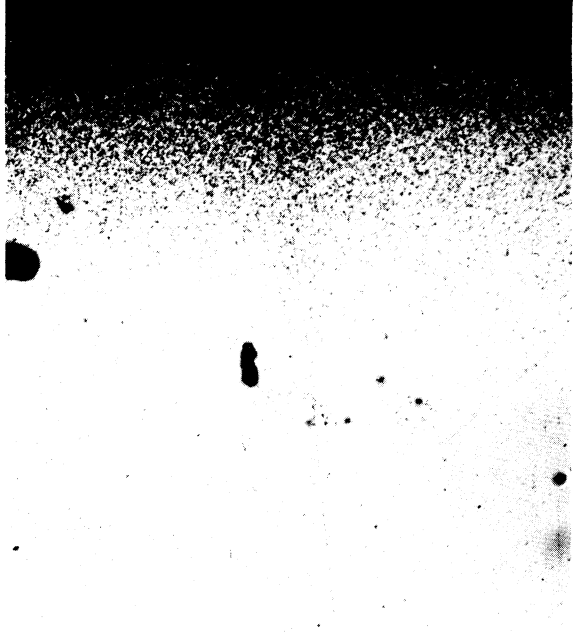

Fig. 32
Diffusion of Nickel Into Copper Bicrystal
At 1700°F ($\Theta = 45^{\circ}$)

Stripping-Film Autoradiograph 250X
Diffusion Time: 27 hrs. Expos. Time: 5 days

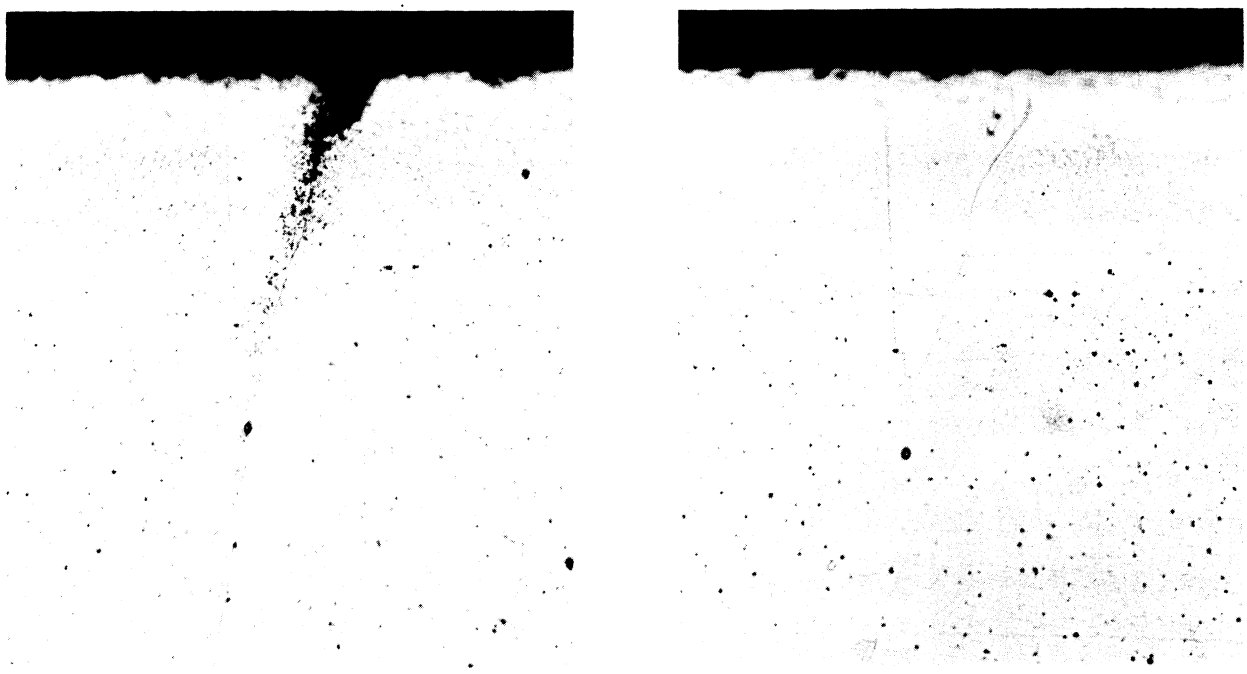

(a) Stripping-Film Autoradiograph 500X (b) Photomicrograph 500X

Fig. 33

Diffusion of Nickel Along Preferred Boundaries of Polycrystalline Copper at 1200°F
Diffusion Time: 120 hrs.
Autorad.Exp.Time: 5 days

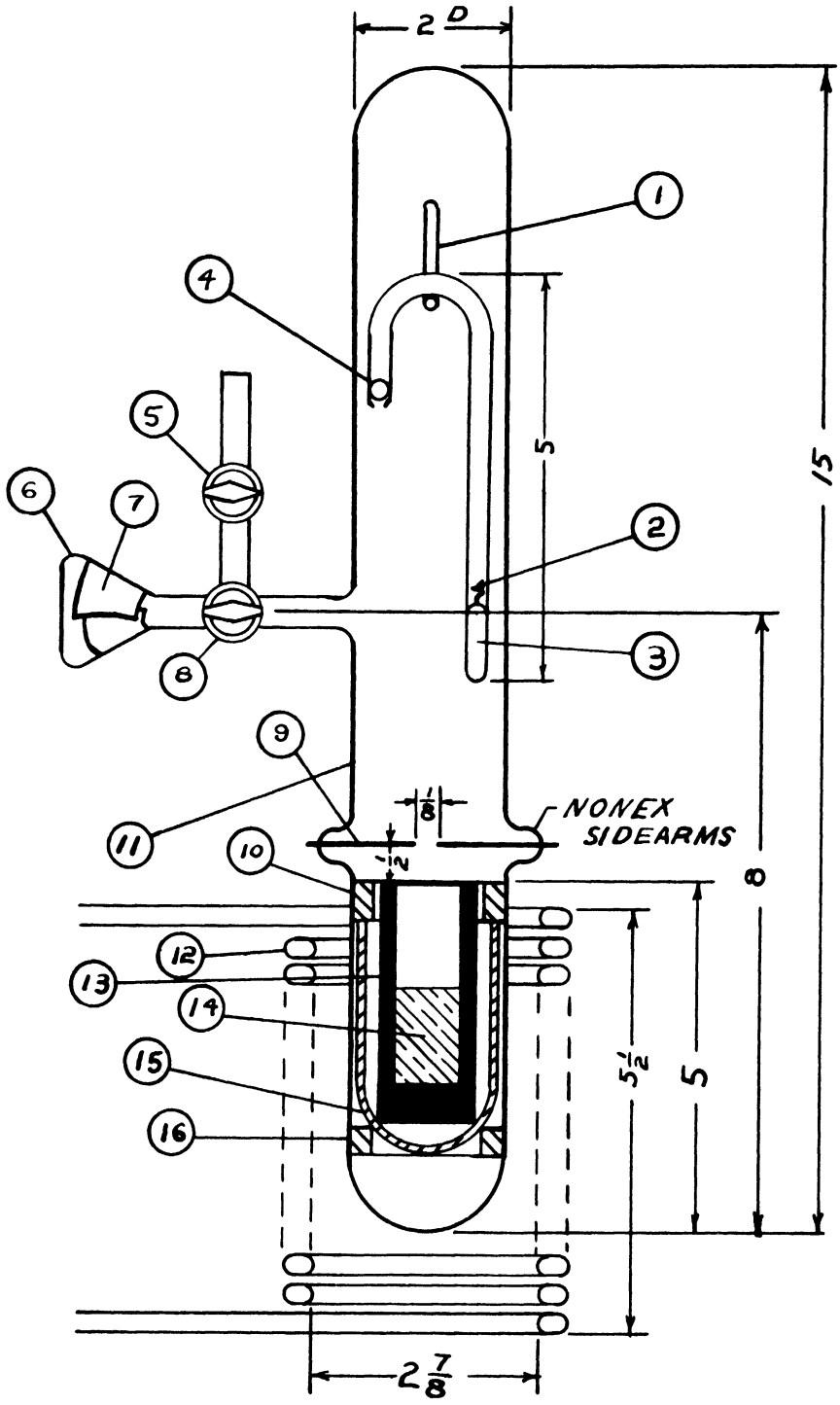

KEY TO FIGURE

1. Glass hook
2. Breakoff tips
3. Tritium capsule in 11-mm tube
4. 1/4-inch diameter steel ball
5. One-way stopcock
6. 25-ml flask
7. Palladium foil, 36 cm^2
8. Three-way perpendicular stopcock
9. 22 gauge tungsten-wire electrodes
10. Alundum ring
11. 2-inch pyrex tube about 1/8 inch thick
12. Induction coil, 20 turns
13. Graphite crucible, 1-3/8 inch O.D. by 1 inch I.D. by 3 inches long by 1/2 inch thick at bottom
14. Bronze charge, 160.5 gm (10% tin)
15. Alundum holder
16. Alundum ring

Note: Mica sheet covers the inside of the 2-inch tube from the bottom to the electrodes.

Scale: 5/12 inch = 1 inch

Fig. 34. Furnace for Melting Copper-Tin Alloys under Tritium Atmosphere

Fig. 35

Typical "Steam" Reaction Microporosity In Copper-Tin Alloy Melted Under Hydrogen (Tritium) Atmosphere.
Photomicrograph Dichromate etch, 500X

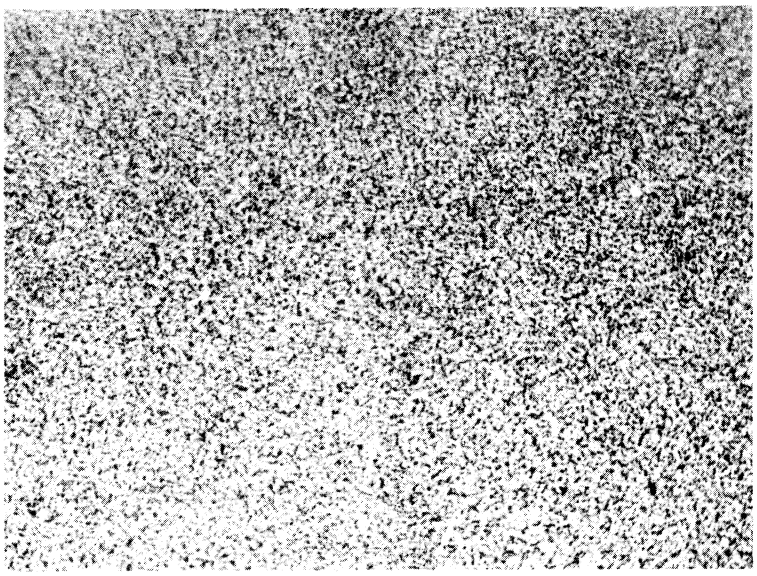

Fig. 36

Contact Autoradiograph Of 93-Copper-7-Tin Alloy Containing Tritium. Area Shown is roughly at center of contact area between specimen and photographic plate.

Expos. Time: 14 days 150X of Autoradiograph

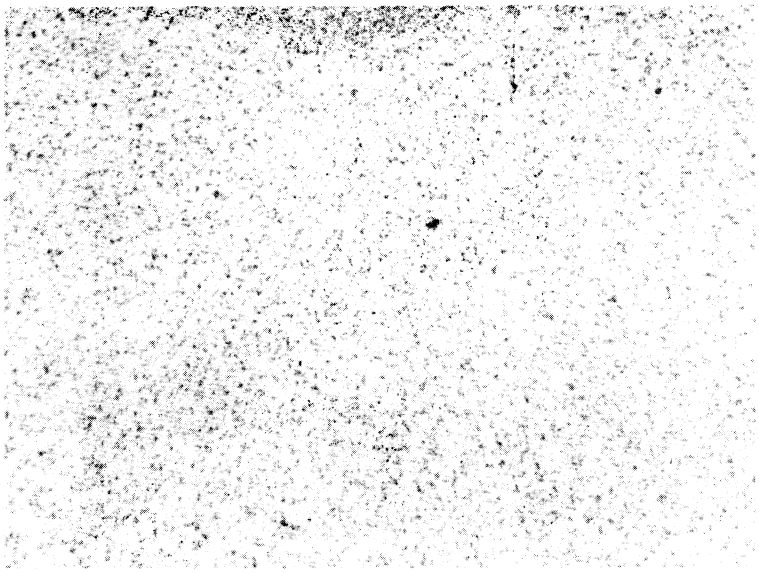

Fig. 37

Contact Autoradiograph Of Specimen and Area Similar to Fig.36 at Higher Magnification.

Expos. Time: 14 days 250X of Autoradiograph

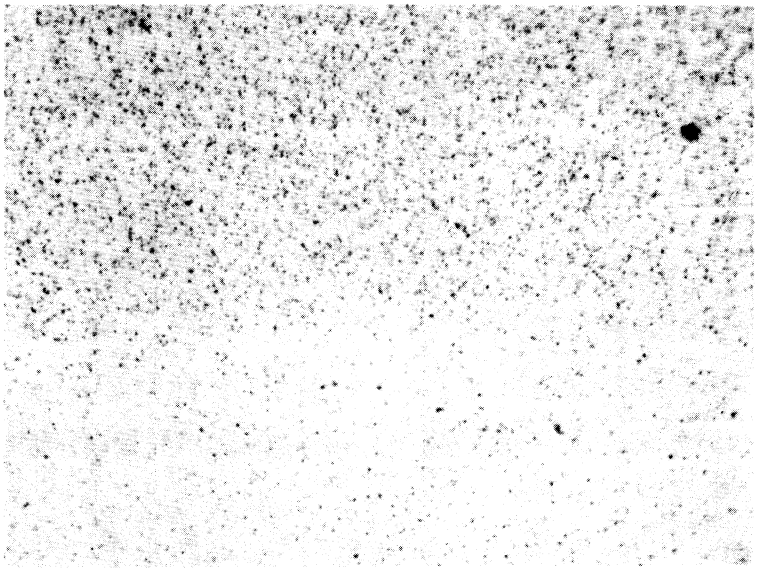

Fig. 38

Contact Autoradiograph Of Copper-Tin Alloy Containing Tritium Showing Edge of Contact Area. Note darkening in area in contact with specimen and little or none in the adjoining area of plate.

Expos. Time: 14 days 250X of Autoradiograph

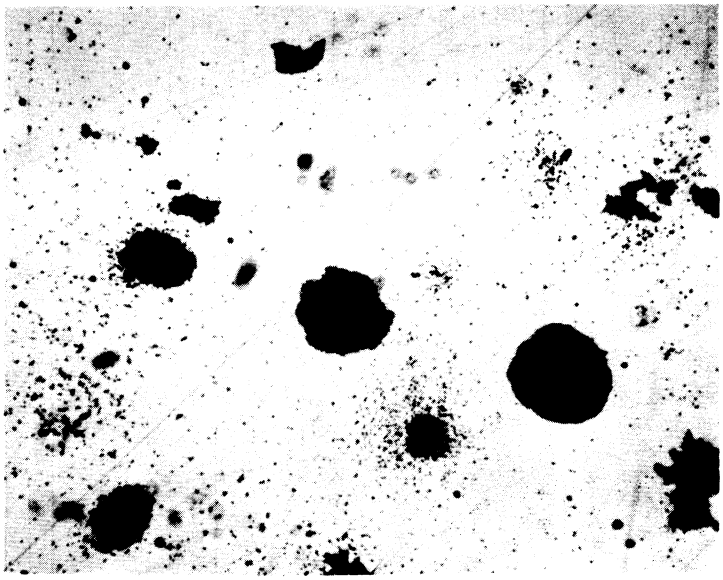

Fig. 39

Autoradiograph Of Cast Iron Made With Radioactive Sulphur Additions.
The black areas are the graphite spherulites.
Stripping-Film Autoradiograph 500X
Expos. Time: 7 days

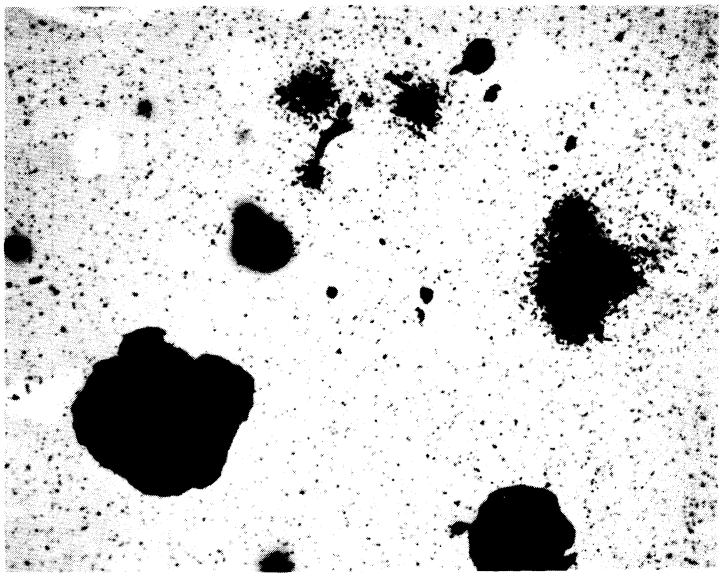

Fig. 40

Control Autoradiograph Of Cast Iron Made With Stable Sulphur Additions.
Note similarity to Fig. 39 in the appearance of response to apparent radioactivity.
Stripping-Film Autoradiograph 500X
Expos. Time: 7 days